

Lecture 5:

Eddies and tropospheric climate

- (i) The observed circulation
- (ii) The troposphere without eddies
- (iii) Tropospheric eddies and waves
- (iv) Baroclinic instability and synoptic eddies
- (v) Synoptic eddy transports
- (vi) Variability: Annular modes

FDEPS 2010
Alan Plumb, MIT
Nov 2010

(i) The observed circulation

observed mean meridional circulation

[Oort & Peixoto]

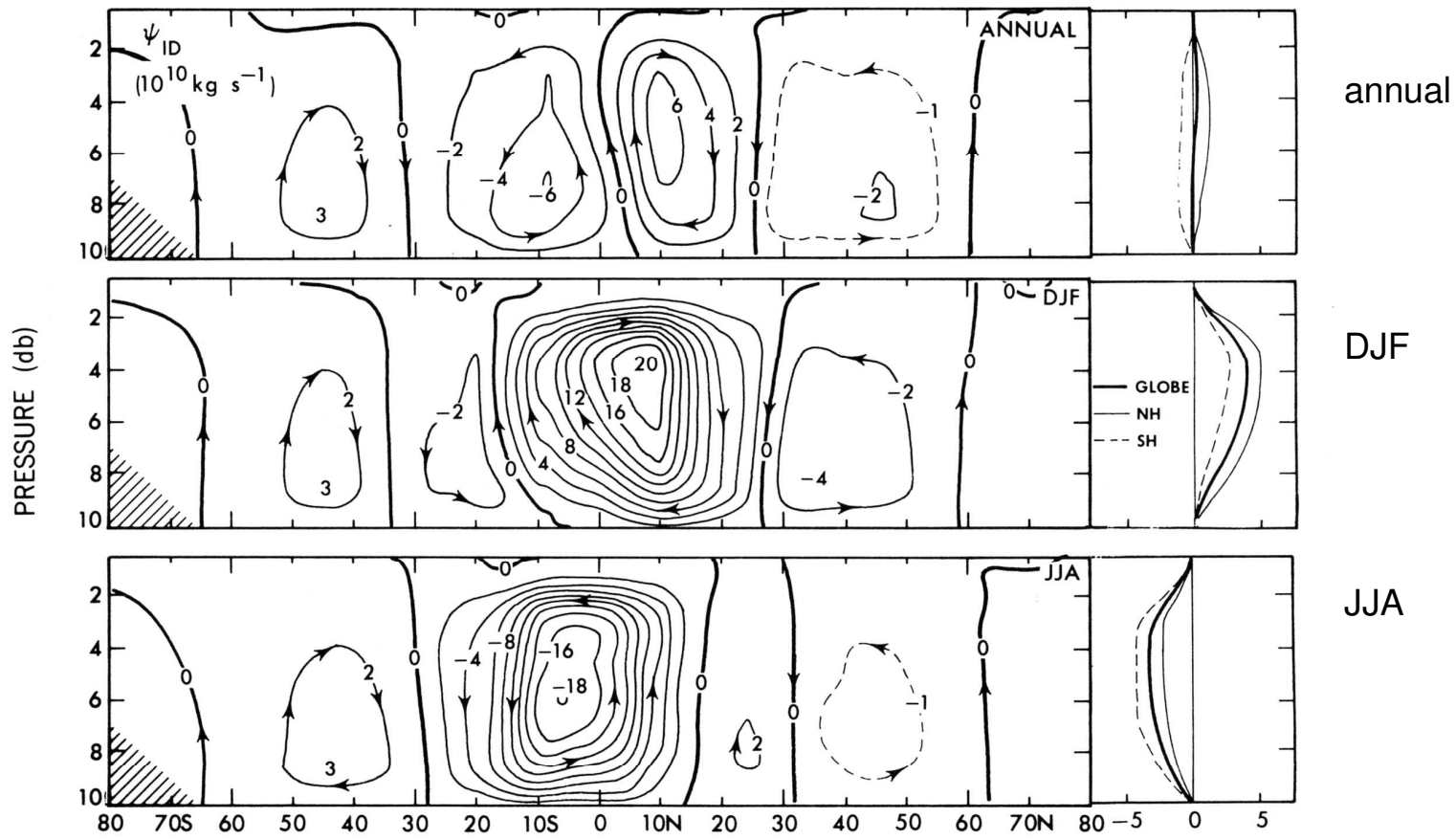


FIGURE 7.19. Zonal-mean cross sections of the mass stream function in $10^{10} \text{ kg s}^{-1}$ for annual, DJF, and JJA mean conditions. Vertical profiles of the hemispheric and global mean values are shown on the right.

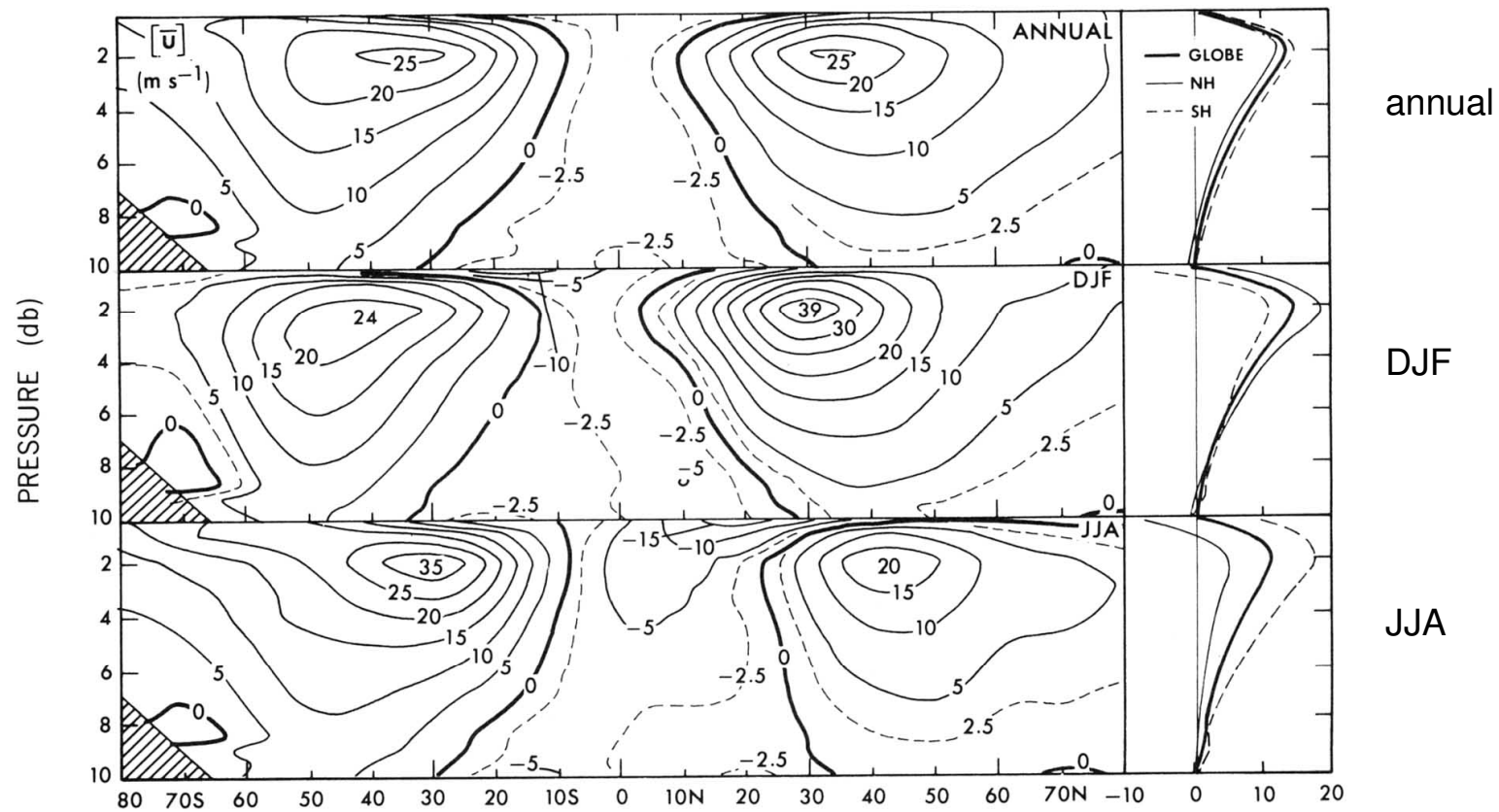
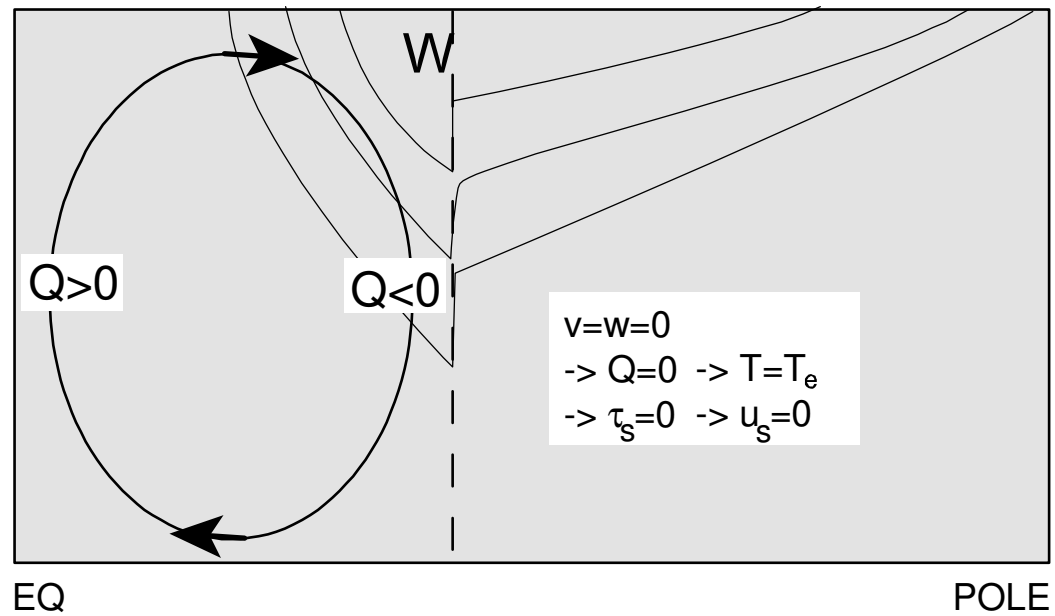


FIGURE 7.15. Zonal-mean cross sections of the zonal wind component in m s^{-1} for annual, DJF, and JJA mean conditions. Vertical profiles of the hemispheric and global mean values are shown on the right.

(ii) The troposphere without eddies

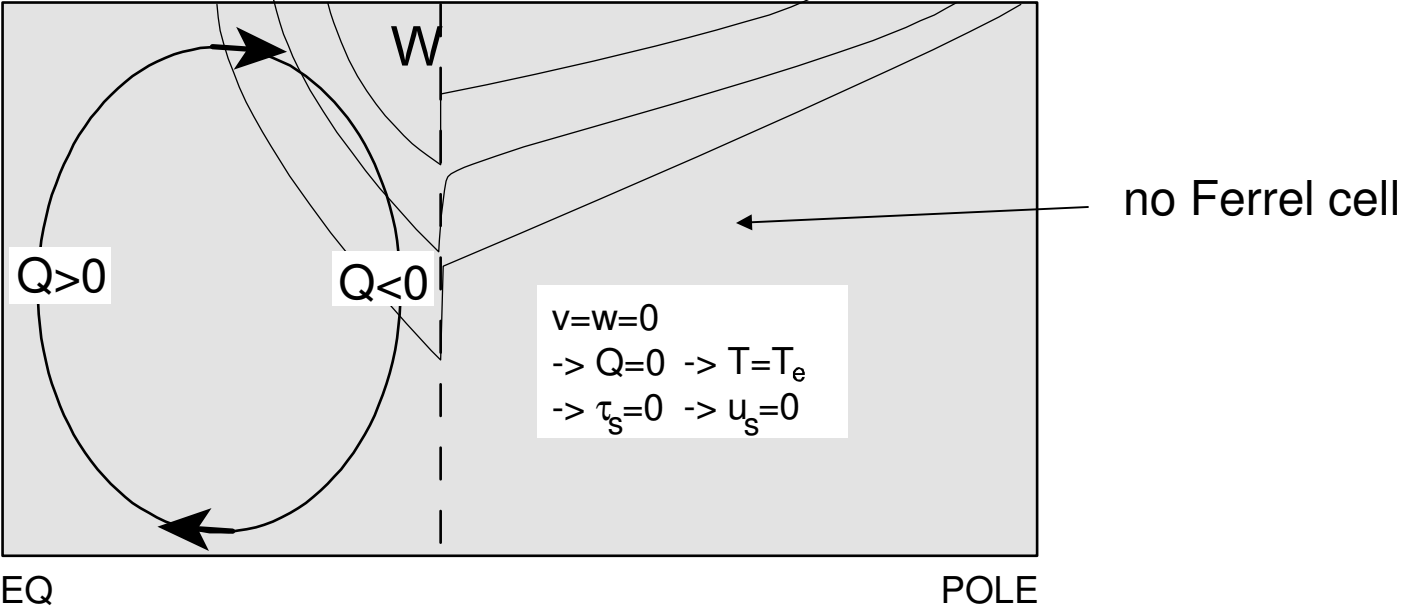
The troposphere without eddies

[Held & Hou, *J Atmos Sci*, 1980]



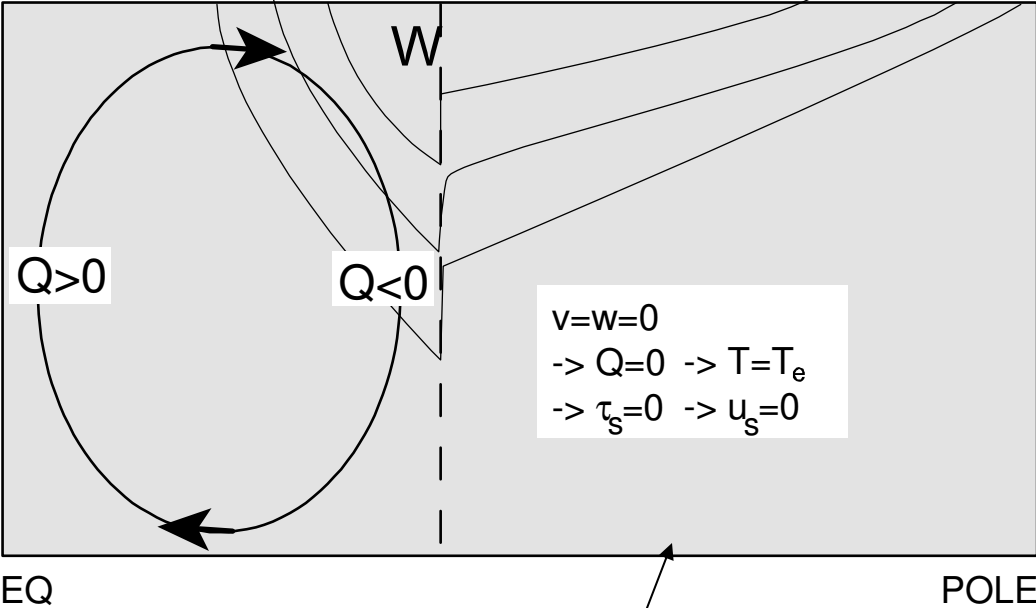
The troposphere without eddies

[Held & Hou, *J Atmos Sci*, 1980]



The troposphere without eddies

[Held & Hou, *J Atmos Sci*, 1980]



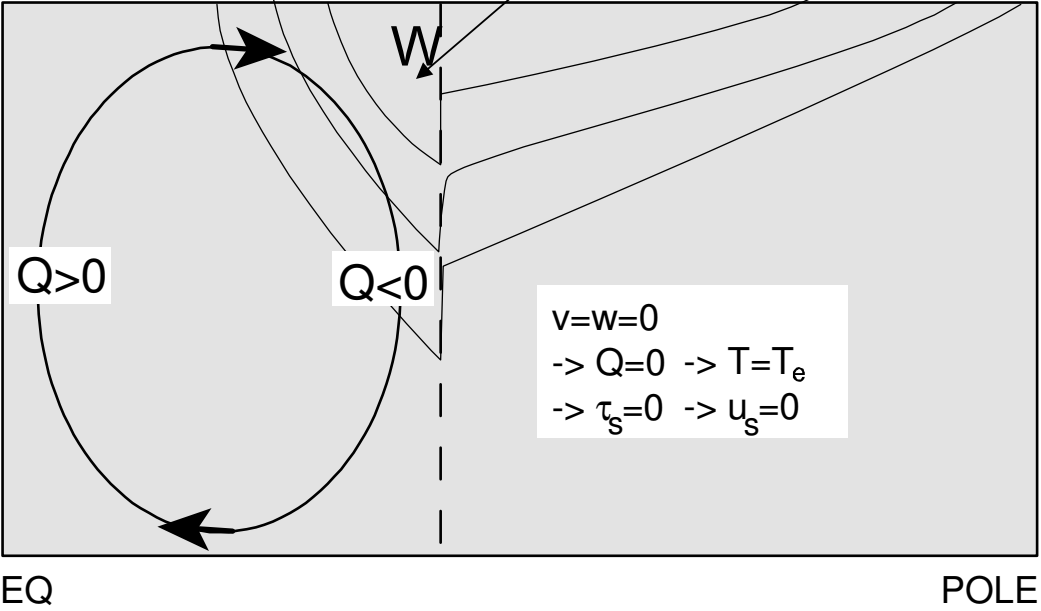
no Ferrel cell

no surface westerlies

The troposphere without eddies

[Held & Hou, *J Atmos Sci*, 1980]

westerly jet much too strong :
temperature gradient too large



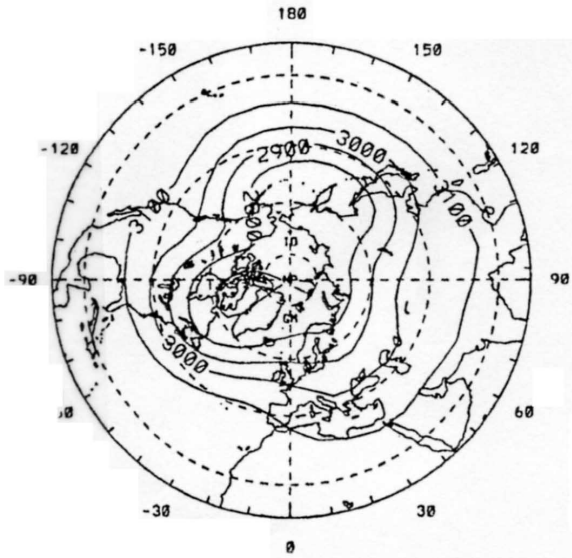
no Ferrel cell

no surface
westerlies

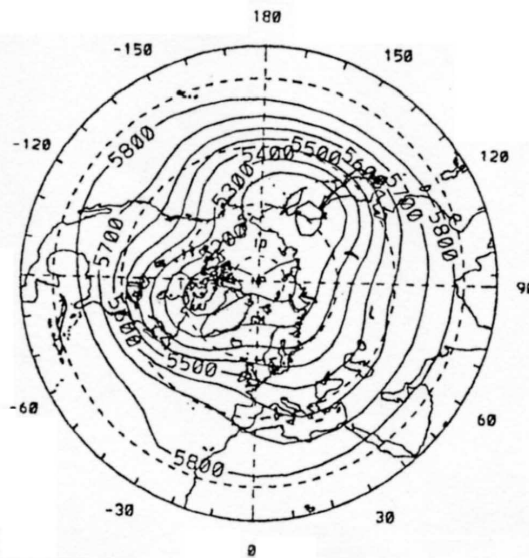
(iii) Tropospheric eddies and waves

Stationary Rossby waves

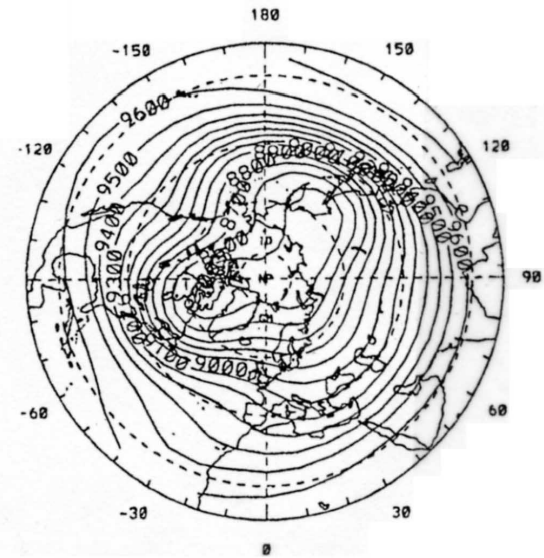
JANUARY NH 700 MB HEIGHT



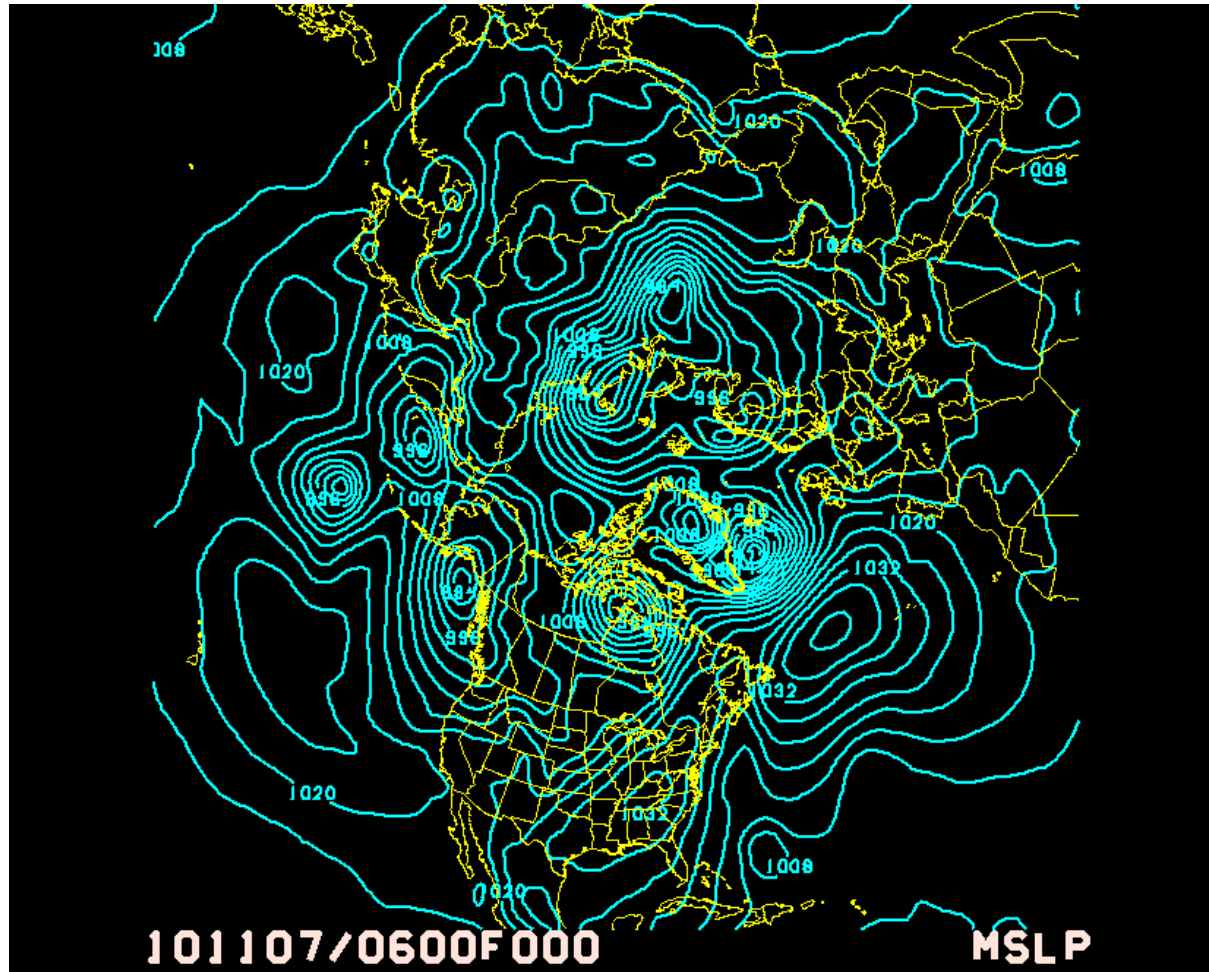
JANUARY NH 500 MB HEIGHT



JANUARY NH 300 MB HEIGHT



Typical surface pressure analysis



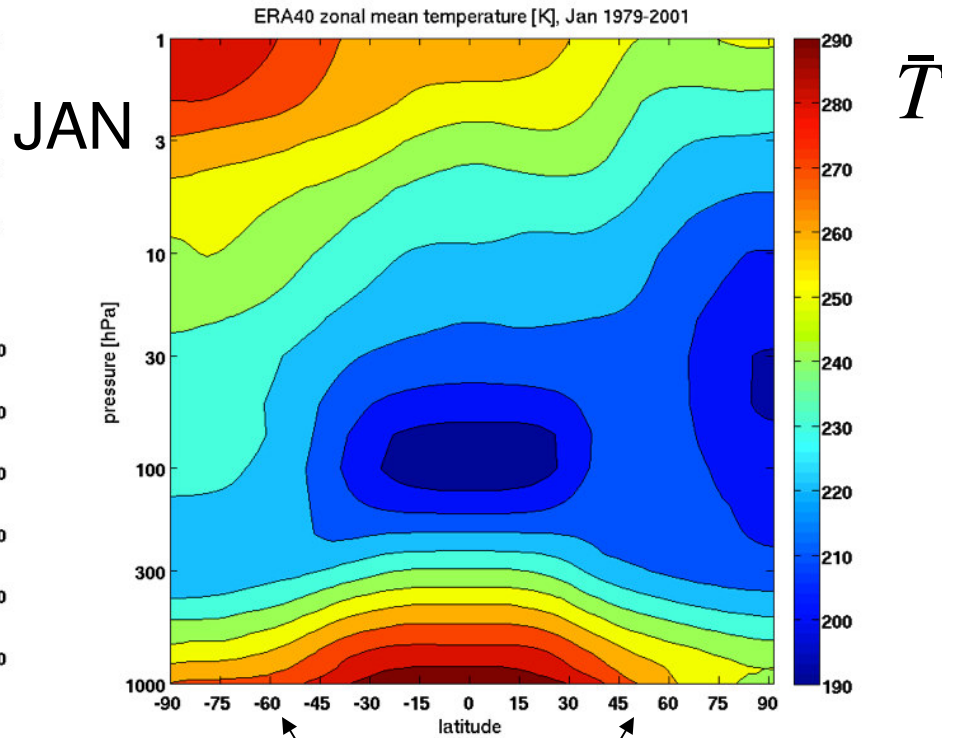
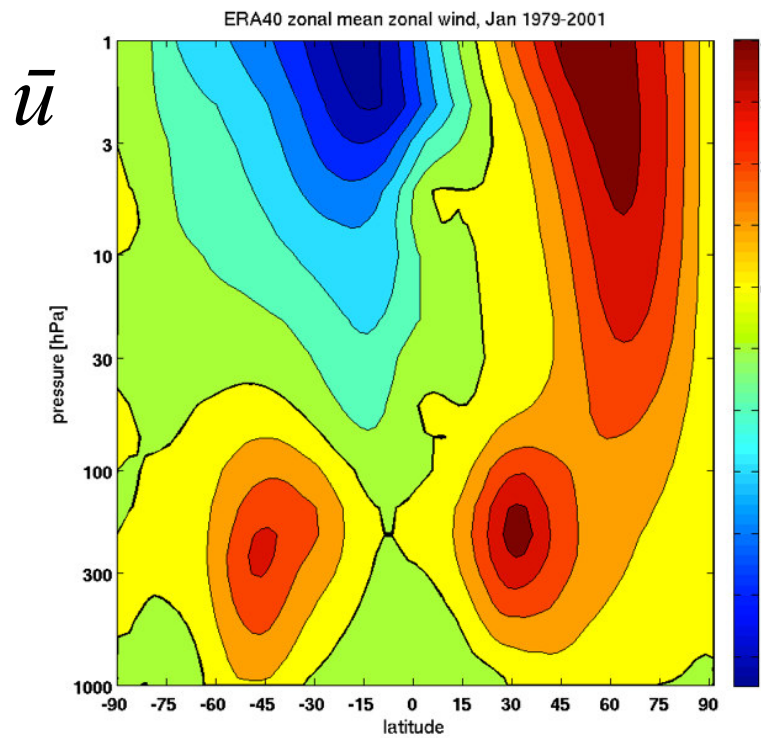
(iv) Baroclinic instability and synoptic eddies

Baroclinic instability

A zonal flow is *stable* to inviscid, adiabatic, quasigeostrophic normal mode perturbations if

- a. there is no change of sign of PV gradient within the fluid and
- b. the system is bounded above and below by isentropic boundaries.

The *Charney-Stern theorem*. (does not apply to non-normal-mode growth).



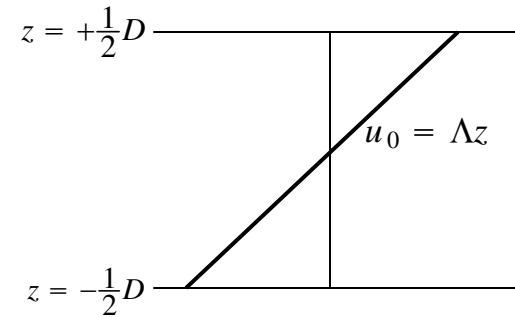
PV gradient (not shown) $\partial \bar{q} / \partial y > 0$ in interior

lower boundary is *not* isentropic

Baroclinic instability: the Eady problem

Simplest example, and relevant to the troposphere

1. Boussinesq ($\rho = \text{constant}$)
2. Inviscid, adiabatic flow on an f -plane ($\beta = 0$)
3. Uniform buoyancy frequency: N^2 constant
4. Rigid upper and lower boundaries at $z = \pm \frac{1}{2}D$, on which $w = 0$.
5. Balanced background zonal flow increasing linearly with height: $u_0 = \Lambda z$



→ linear latitudinal temperature gradient:

$$\frac{\partial}{\partial y} \left(\frac{T_0}{T_*} \right) = \frac{f_0}{g} \frac{\partial u_0}{\partial z} = \frac{f_0 \Lambda}{g}$$

→ no basic state QGPV gradient:

$$\frac{\partial q_0}{\partial y} = -\frac{\partial^2 u_0}{\partial y^2} - \frac{f_0^2}{N^2} \frac{\partial^2 u_0}{\partial z^2} = 0$$

$$\left(\frac{\partial}{\partial t} + u_0 \frac{\partial}{\partial x} \right) q' + v' \frac{\partial q_0}{\partial y} = \left(\frac{\partial}{\partial t} + u_0 \frac{\partial}{\partial x} \right) q' = 0 \quad \rightarrow \quad q' = 0$$

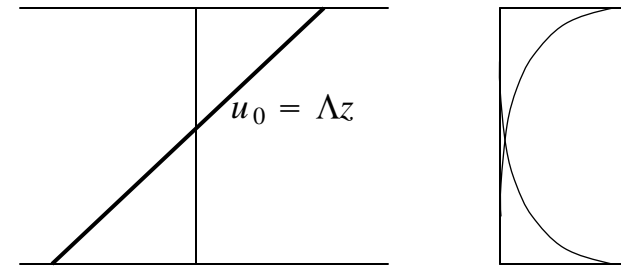
$$\rightarrow q' = \frac{\partial^2 \psi'}{\partial x^2} + \frac{\partial^2 \psi'}{\partial y^2} + \frac{f_0^2}{N^2} \frac{\partial^2 \psi'}{\partial z^2} = 0$$

Look for separable modal, wave-like solutions $\psi' = \text{Re}[\Phi(z)e^{i(kx+ly-ckt)}]$
then

$$\frac{d^2 \Phi}{dz^2} - \frac{N^2}{f_0^2} \kappa^2 \Phi = 0$$

where $\kappa = \sqrt{k^2 + l^2}$. Then $\Phi \sim \exp(\pm N\kappa z/f_0)$, or

$$\Phi(z) = A \cosh\left(\frac{N\kappa}{f_0} z\right) + B \sinh\left(\frac{N\kappa}{f_0} z\right)$$



→ boundary trapped

On upper and lower boundaries $z = \pm D/2$, $w' = 0$

$$\rightarrow \left(\frac{\partial}{\partial t} + u_0 \frac{\partial}{\partial x} \right) T' + \frac{\partial \psi'}{\partial x} \frac{\partial T_0}{\partial y} = 0$$

$$\rightarrow (U - c) \frac{d\Phi}{dz} - \Lambda \Phi = 0.$$

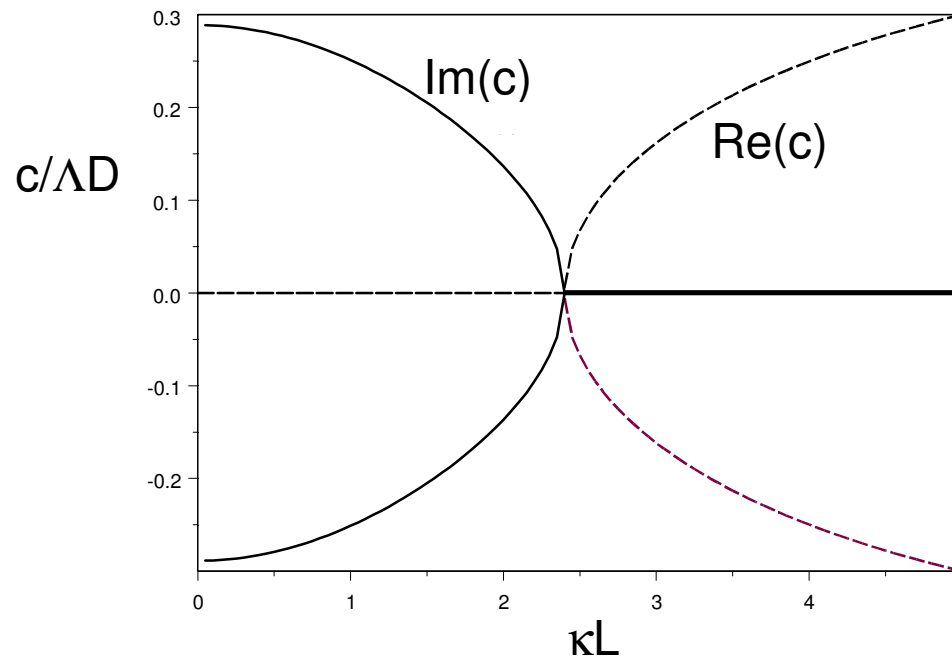
$L = ND/f_0$
internal radius of deformation

After much manipulation, find

$$c = \pm \frac{\Lambda D}{\kappa L} \sqrt{\left[\frac{\kappa L}{2} - \tanh\left(\frac{1}{2}\kappa L\right) \right] \left[\frac{\kappa L}{2} - \coth\left(\frac{1}{2}\kappa L\right) \right]}$$

$$\frac{c}{\Lambda D} = \pm \frac{1}{\kappa L} \sqrt{\left[\frac{\kappa L}{2} - \tanh\left(\frac{1}{2}\kappa L\right) \right] \left[\frac{\kappa L}{2} - \coth\left(\frac{1}{2}\kappa L\right) \right]}$$

short waves, $\kappa L < 2.3994$: $c^2 > 0$: propagating boundary waves, no growth
 long waves, $\kappa L > 2.3994$: $c^2 < 0$: nonpropagating, exponential growth



$$\frac{c}{\Delta D} = \pm \frac{1}{\kappa L} \sqrt{\left[\frac{\kappa L}{2} - \tanh\left(\frac{1}{2}\kappa L\right) \right] \left[\frac{\kappa L}{2} - \coth\left(\frac{1}{2}\kappa L\right) \right]}$$

short waves, $\kappa L < 2.3994$: $c^2 > 0$: propagating boundary waves, no growth
 long waves, $\kappa L > 2.3994$: $c^2 < 0$: nonpropagating, exponential growth

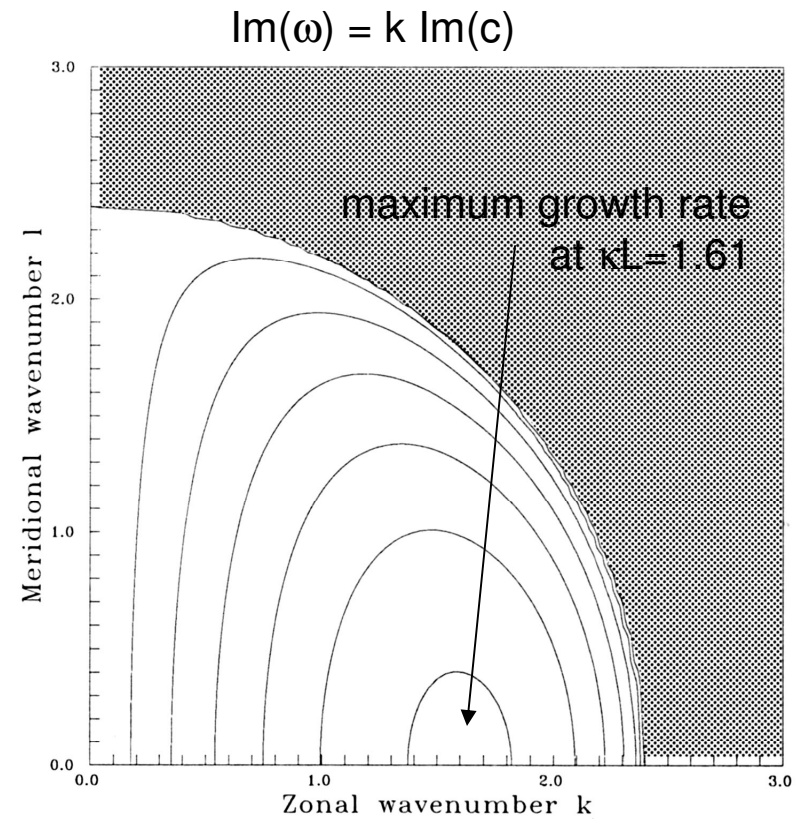
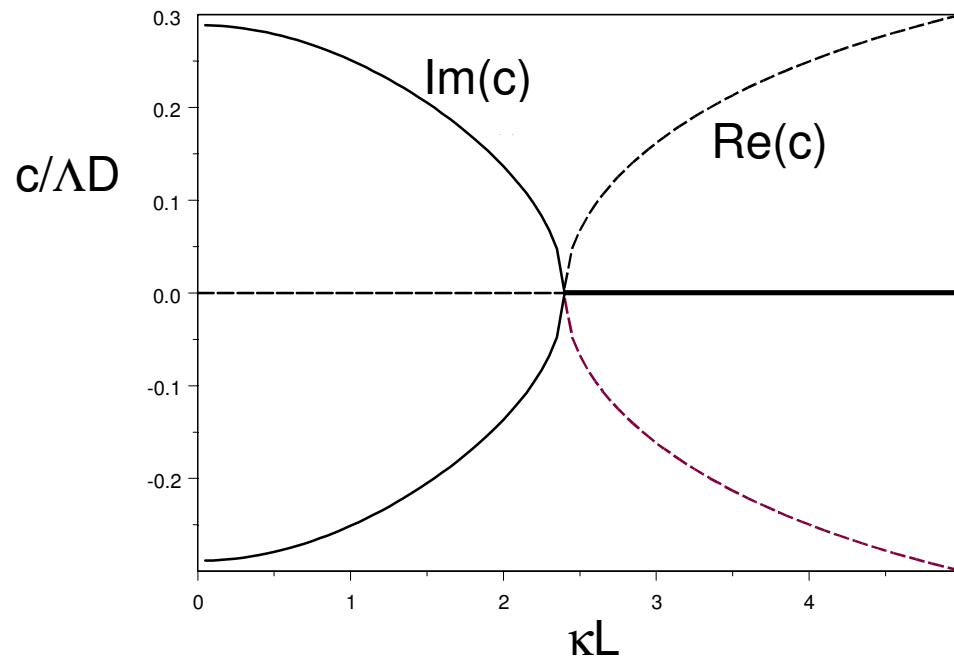
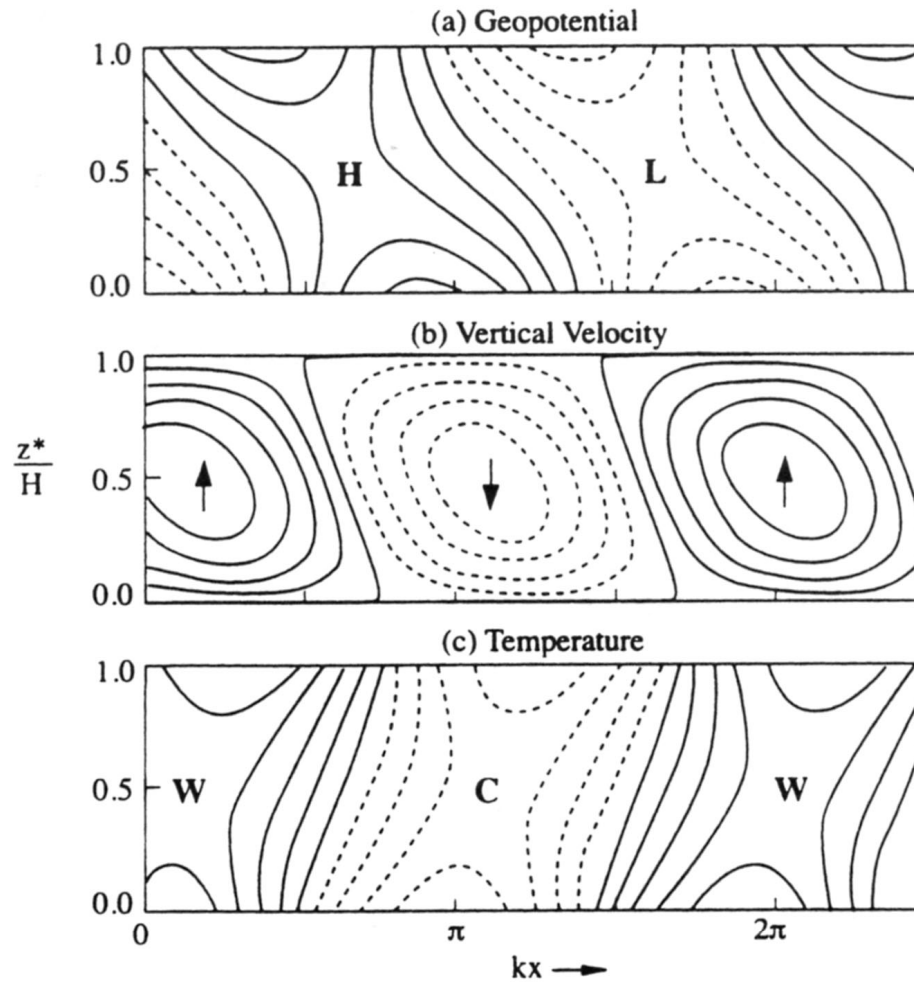


Fig. 5.17. Growth rate of waves with zonal wavenumber k and meridional wavenumber l according to the Eady model of baroclinic instability. Contour interval $0.05 K_R \Delta U$. [James]

Structure of fastest growing wave:



Note.:

$$\overline{w'T'} > 0$$

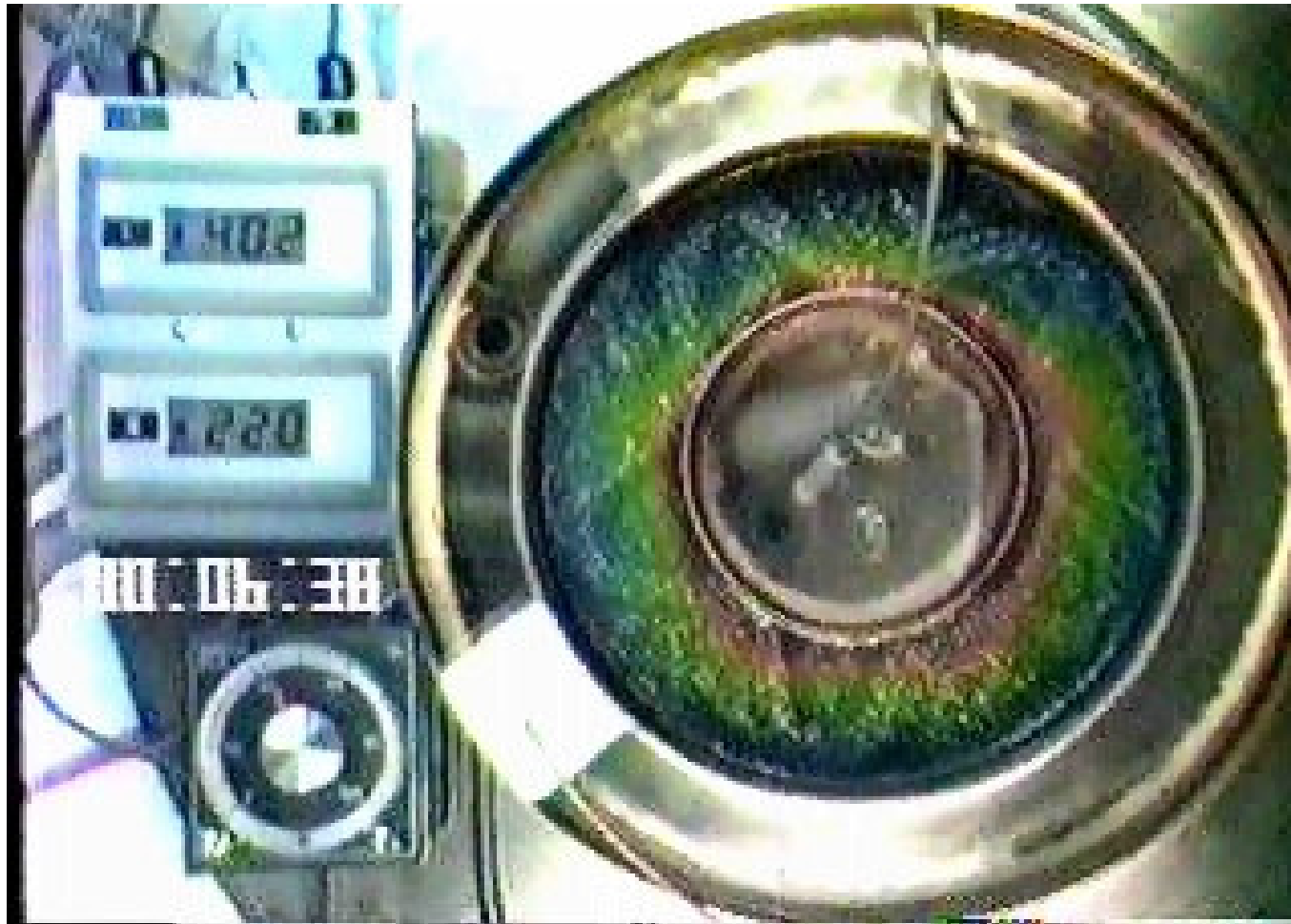
$\overline{v'T'}$ is poleward

Fig. 8.10 Properties of the most unstable Eady wave. (a) Contours of perturbation geopotential height; *H* and *L* designate ridge and trough axes, respectively. (b) Contours of vertical velocity; up and down arrows designate axes of maximum upward and downward motion, respectively. (c) Contours of perturbation temperature; *W* and *C* designate axes of warmest and coldest temperatures, respectively. In all panels 1 and 1/4 wavelengths are shown for clarity.

[Holton]

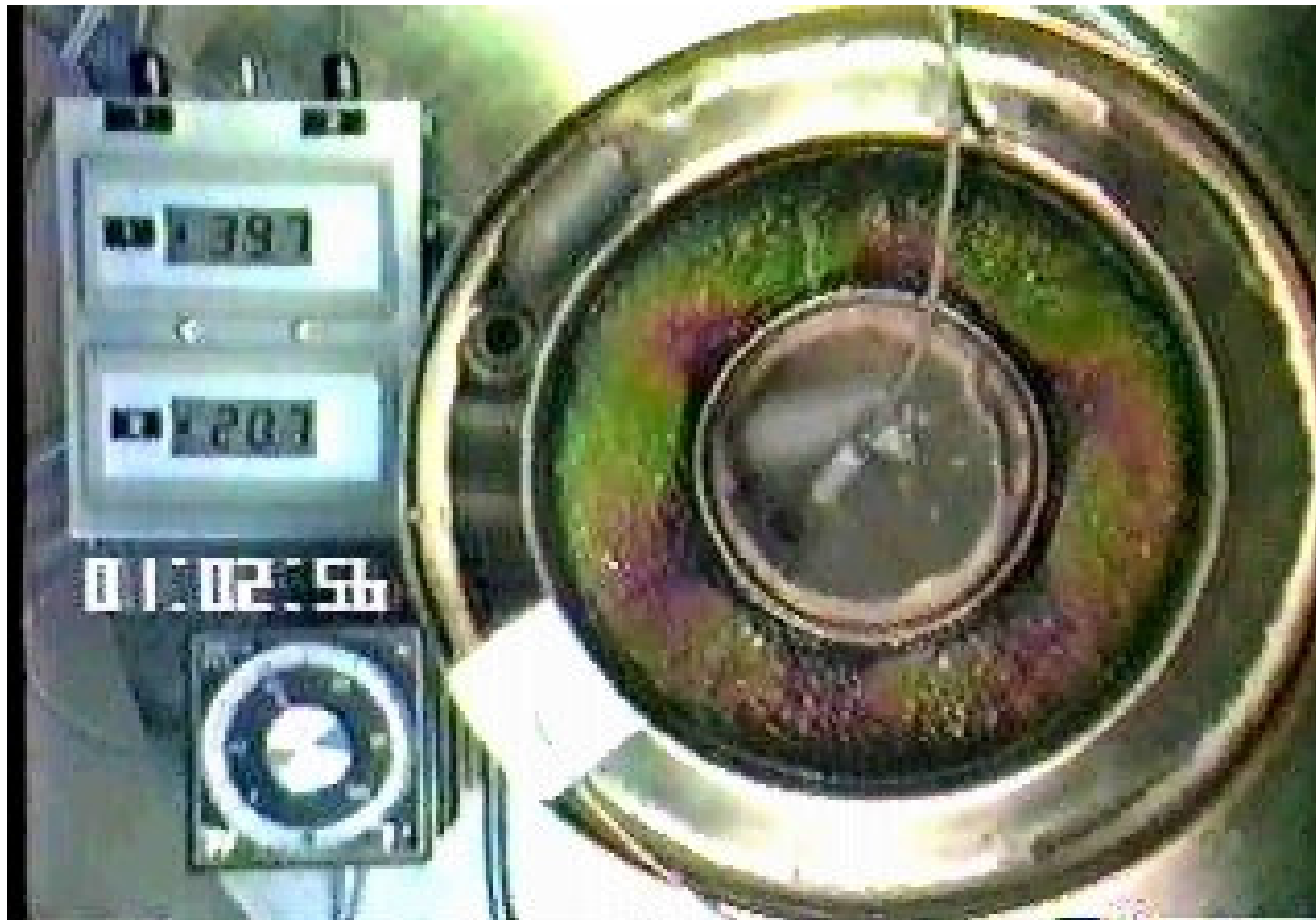
実験室の中の空と海

Atmosphere and Ocean
in a Laboratory



実験室の中の空と海

Atmosphere and Ocean
in a Laboratory



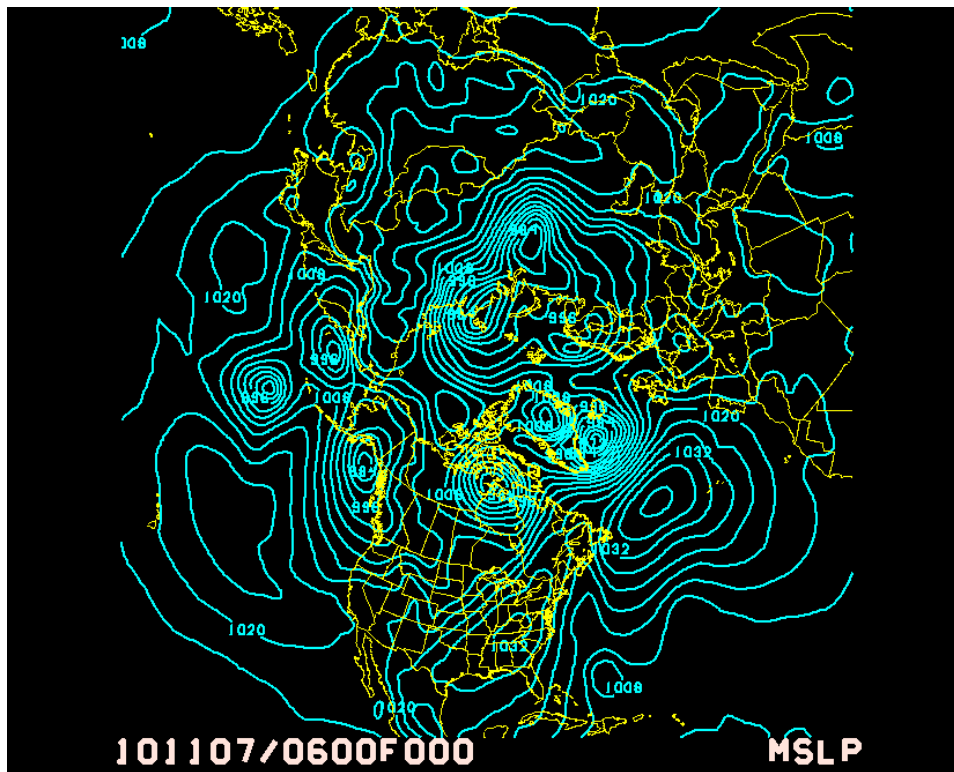
Baroclinic instability in the atmosphere:

Typical values in midlatitude troposphere

$D \simeq 10\text{km}$, $N \simeq 1 \times 10^{-2}\text{s}^{-1}$, $f_0 \simeq 1.0 \times 10^{-4}\text{s}^{-1}$, $\Lambda \simeq 2.5 \times 10^{-3}\text{s}^{-1}$.

So the fastest growth rate is $6.5 \times 10^{-6}\text{s}^{-1}$, \rightarrow e -folding time $1.5 \times 10^5\text{s} \simeq 1.8$ days.

Wavenumber of the fastest growing wave is $1.61f_0/ND \simeq 1.61 \times 10^{-6}\text{m}^{-1}$,
giving wavelength $2\pi/k \simeq 3900$ km. (At 45° , corresponds to zonal wavenumber 7.)



(v) Synoptic eddy transport

\mathbf{F} , $\nabla \cdot \mathbf{F}$ in troposphere
[Oort & Peixoto]

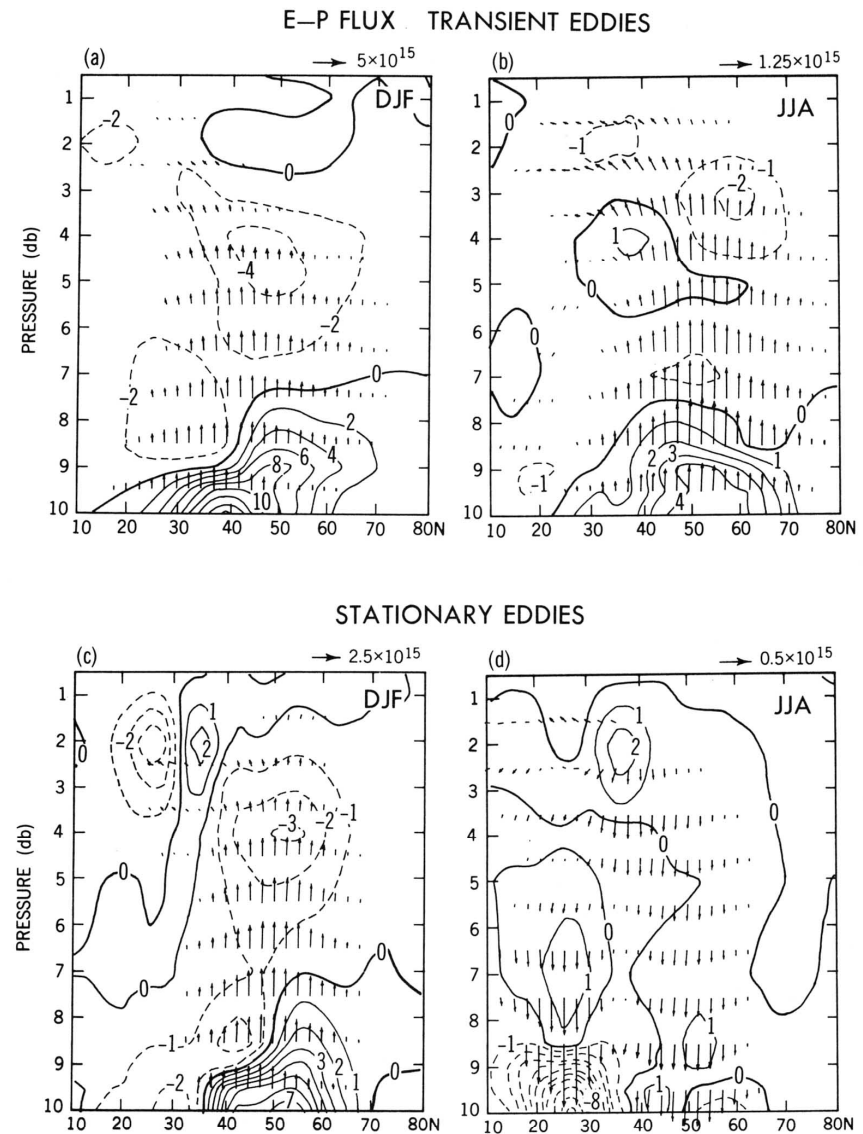
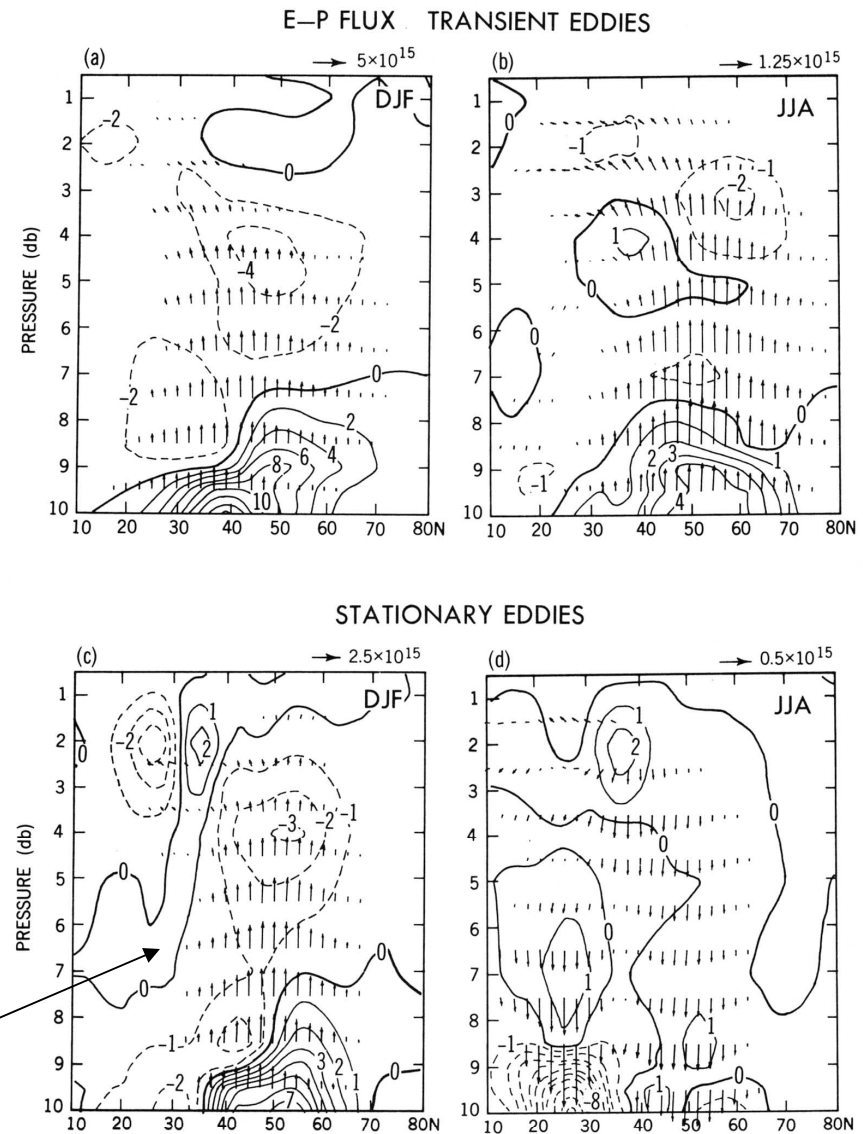


FIGURE 14.9 Cross sections of the Eliassen-Palm flux vectors $\hat{\mathbf{F}}$ plotted as arrows and of their divergence given by solid (positive) and dashed (negative) contours. Shown are the transient eddy (upper panel) and stationary eddy components (lower panel) of the E - P fluxes for mean northern winter and summer conditions for the period 1963–1973. Contour intervals are $2 \times 10^{15} \text{ m}^3$ for the transient eddy winter case and $1 \times 10^{15} \text{ m}^3$ for the other cases. The arrows are scaled differently in the various diagrams as indicated in the upper right-hand corner of each diagram. Each scale represents the value of the horizontal component \hat{F}_ϕ in m^3 . The scale for the vertical component \hat{F}_p is equal to the scale for \hat{F}_ϕ , but multiplied by 62.2 kPa (1 kPa = 10 mb), so that \hat{F}_p is then in units of $\text{m}^3 \text{ kPa}$.

\mathbf{F} , $\nabla \cdot \mathbf{F}$ in troposphere
[Oort & Peixoto]



stationary waves in winter:
upward propagating from
surface and near-surface
sources

FIGURE 14.9 Cross sections of the Eliassen-Palm flux vectors $\hat{\mathbf{F}}$ plotted as arrows and of their divergence given by solid (positive) and dashed (negative) contours. Shown are the transient eddy (upper panel) and stationary eddy components (lower panel) of the E - P fluxes for mean northern winter and summer conditions for the period 1963–1973. Contour intervals are $2 \times 10^{15} \text{ m}^3$ for the transient eddy winter case and $1 \times 10^{15} \text{ m}^3$ for the other cases. The arrows are scaled differently in the various diagrams as indicated in the upper right-hand corner of each diagram. Each scale represents the value of the horizontal component \hat{F}_ϕ in m^3 . The scale for the vertical component \hat{F}_p is equal to the scale for \hat{F}_ϕ but multiplied by 62.2 kPa (1 kPa = 10 mb), so that \hat{F}_p is then in units of $\text{m}^3 \text{ kPa}$.

$\mathbf{F}, \nabla \cdot \mathbf{F}$ in troposphere
[Oort & Peixoto]

transient baroclinic eddies also
upward propagating, because
 $\overline{v'T'}$ is poleward

$$F(z) = f \frac{\overline{v'T'}}{\partial \bar{\theta} / \partial z} > 0$$

stationary waves in winter:
upward propagating from
surface and near-surface
sources

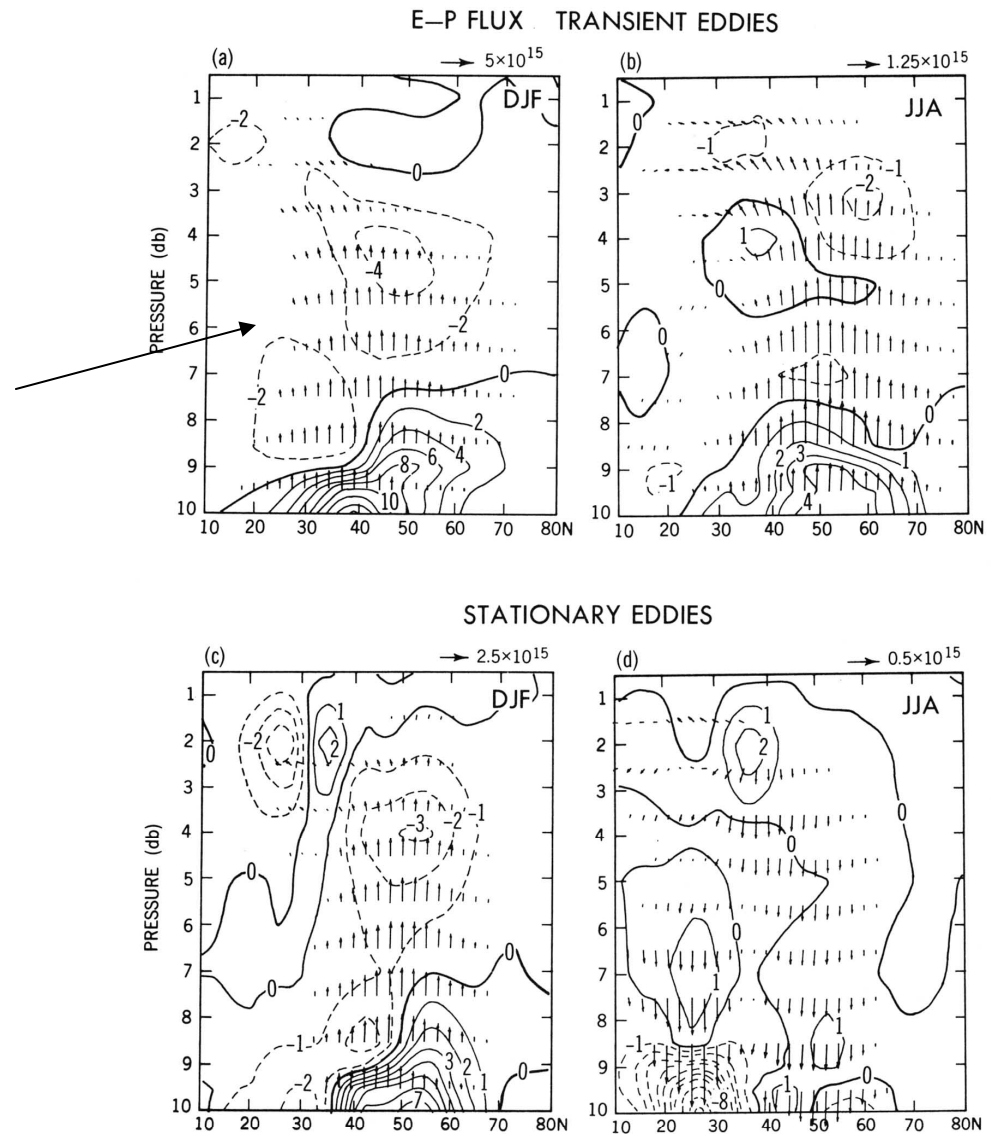


FIGURE 14.9 Cross sections of the Eliassen-Palm flux vectors $\hat{\mathbf{F}}$ plotted as arrows and of their divergence given by solid (positive) and dashed (negative) contours. Shown are the transient eddy (upper panel) and stationary eddy components (lower panel) of the $E-P$ fluxes for mean northern winter and summer conditions for the period 1963–1973. Contour intervals are $2 \times 10^{15} \text{ m}^3$ for the transient eddy winter case and $1 \times 10^{15} \text{ m}^3$ for the other cases. The arrows are scaled differently in the various diagrams as indicated in the upper right-hand corner of each diagram. Each scale represents the value of the horizontal component \hat{F}_ϕ in m^3 . The scale for the vertical component \hat{F}_p is equal to the scale for \hat{F}_ϕ but multiplied by 62.2 kPa (1 kPa = 10 mb), so that \hat{F}_p is then in units of $\text{m}^3 \text{ kPa}$.

\mathbf{F} , $\nabla \cdot \mathbf{F}$ in troposphere
[Oort & Peixoto]

transient baroclinic eddies also
upward propagating, because
 $\overline{v'T'}$ is poleward

$$F(z) = f \frac{\overline{v'T'}}{\partial \bar{\theta} / \partial z} > 0$$

\mathbf{F} *divergent* near (and at) surface;
generally *convergent* in middle and upper
troposphere

stationary waves in winter:
upward propagating from
surface and near-surface
sources

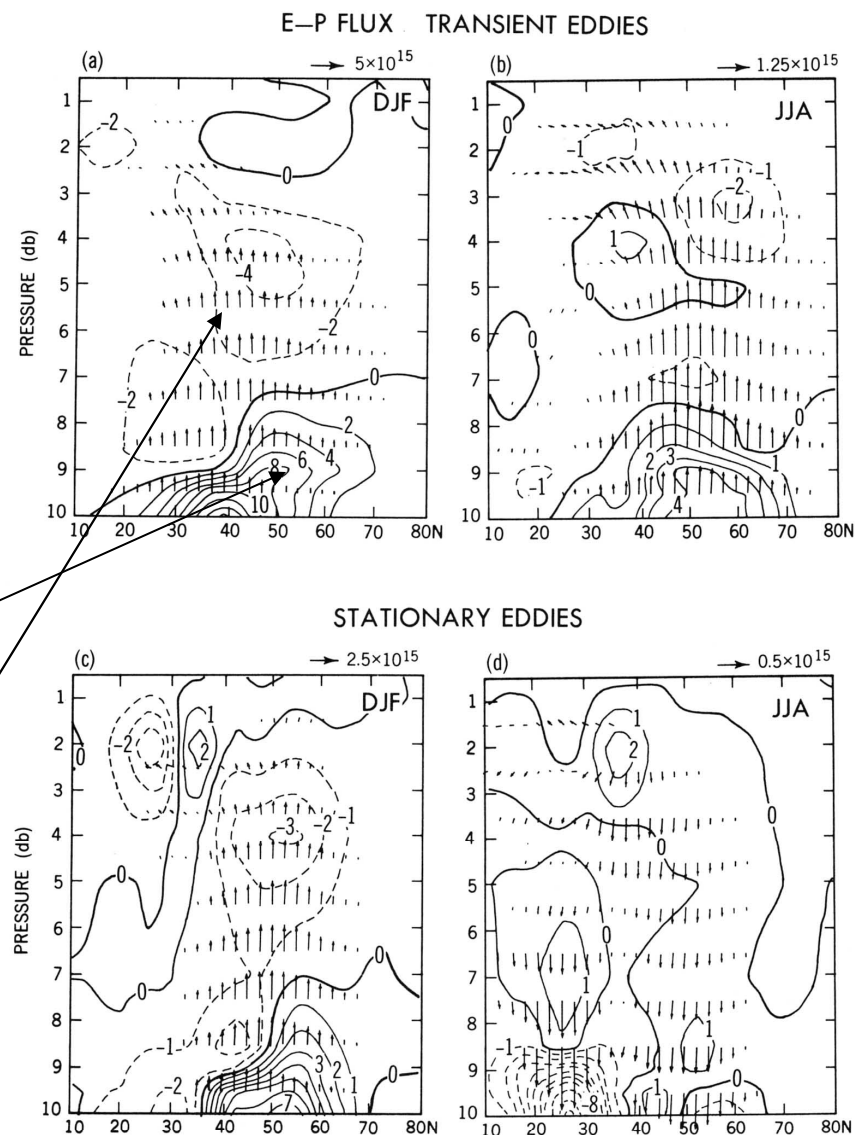
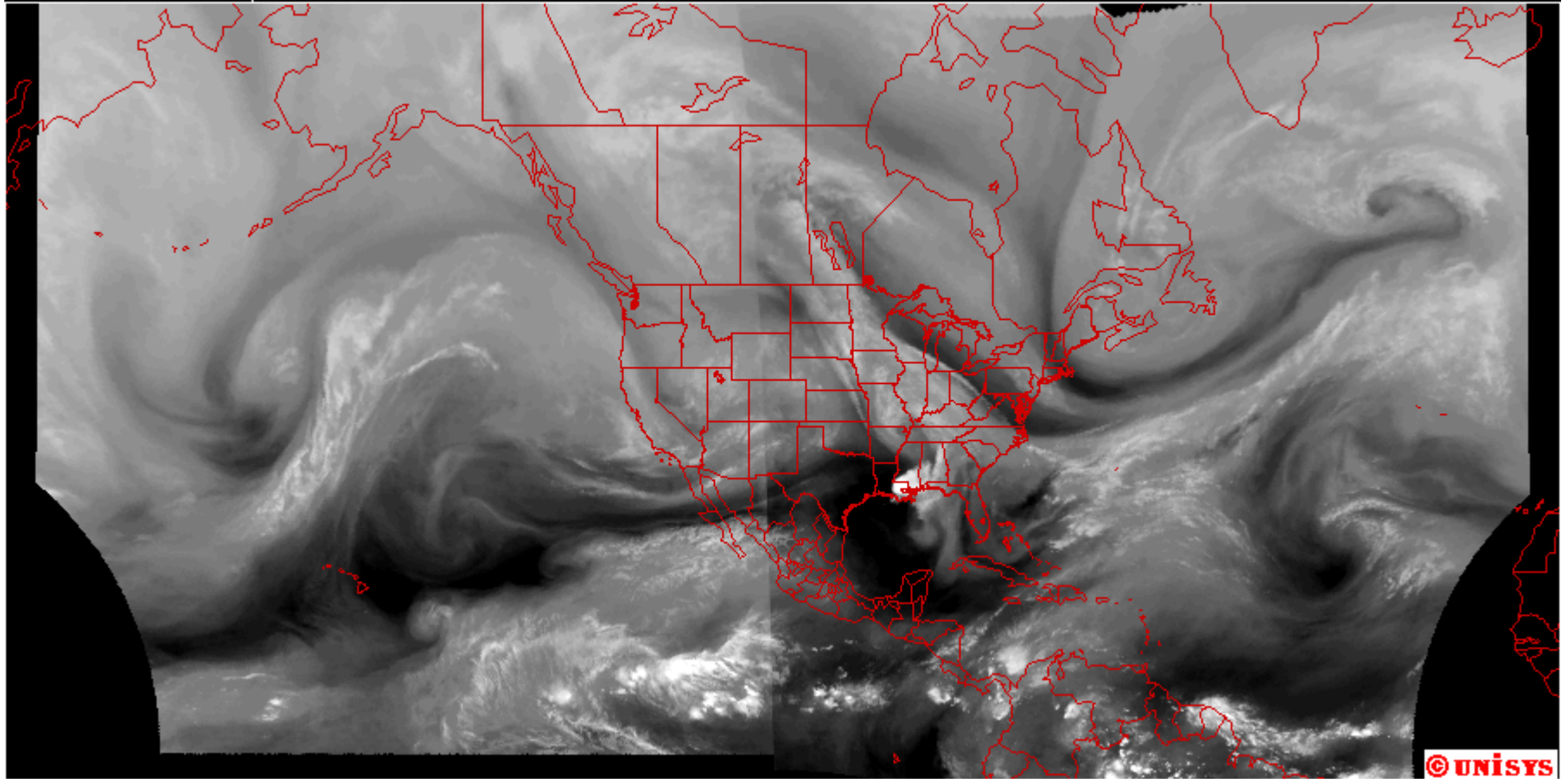


FIGURE 14.9 Cross sections of the Eliassen-Palm flux vectors $\hat{\mathbf{F}}$ plotted as arrows and of their divergence given by solid (positive) and dashed (negative) contours. Shown are the transient eddy (upper panel) and stationary eddy components (lower panel) of the $E-P$ fluxes for mean northern winter and summer conditions for the period 1963–1973. Contour intervals are $2 \times 10^{15} \text{ m}^3$ for the transient eddy winter case and $1 \times 10^{15} \text{ m}^3$ for the other cases. The arrows are scaled differently in the various diagrams as indicated in the upper right-hand corner of each diagram. Each scale represents the value of the horizontal component \hat{F}_ϕ in m^3 . The scale for the vertical component \hat{F}_p is equal to the scale for \hat{F}_ϕ but multiplied by 62.2 kPa (1 kPa = 10 mb), so that \hat{F}_p is then in units of $\text{m}^3 \text{ kPa}$.

GOES NH Water Vapor

1630Z 4 MAY 07



© UNISYS

$\mathbf{F}, \nabla \cdot \mathbf{F}$ in troposphere
[Oort & Peixoto]

transient baroclinic eddies also
upward propagating, because
 $\overline{v'T'}$ is poleward

$$F(z) = f \frac{\overline{v'T'}}{\partial \bar{\theta} / \partial z} > 0$$

note equatorward propagation
in upper troposphere

stationary waves in winter:
upward propagating from
surface and near-surface
sources

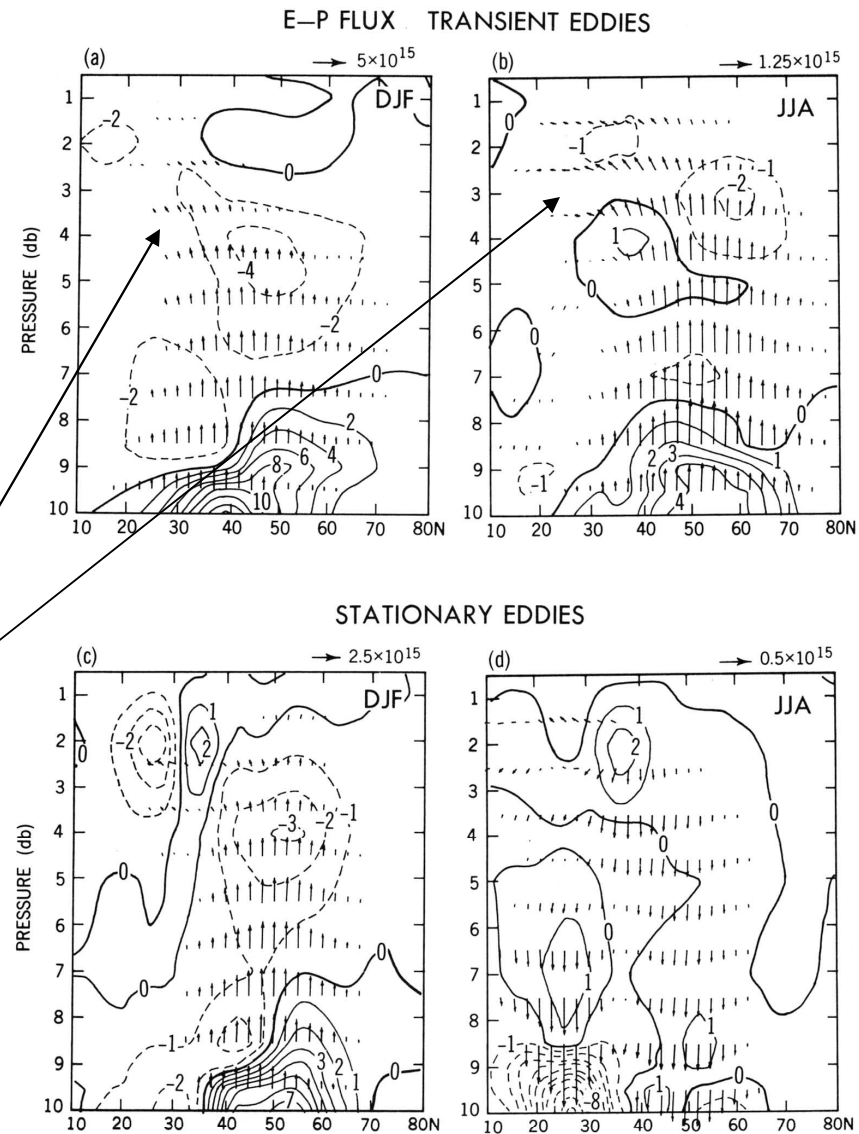


FIGURE 14.9 Cross sections of the Eliassen-Palm flux vectors $\hat{\mathbf{F}}$ plotted as arrows and of their divergence given by solid (positive) and dashed (negative) contours. Shown are the transient eddy (upper panel) and stationary eddy components (lower panel) of the $E-P$ fluxes for mean northern winter and summer conditions for the period 1963–1973. Contour intervals are $2 \times 10^{15} \text{ m}^3$ for the transient eddy winter case and $1 \times 10^{15} \text{ m}^3$ for the other cases. The arrows are scaled differently in the various diagrams as indicated in the upper right-hand corner of each diagram. Each scale represents the value of the horizontal component \hat{F}_ϕ in m^3 . The scale for the vertical component \hat{F}_p is equal to the scale for \hat{F}_ϕ , but multiplied by 62.2 kPa (1 kPa = 10 mb), so that \hat{F}_p is then in units of $\text{m}^3 \text{ kPa}$.

annual mean $\overline{v'T'}$:
 transient eddies dominate, but
 stationary waves contribute in
 northern hemisphere (especially winter)

[Oort & Peixoto]

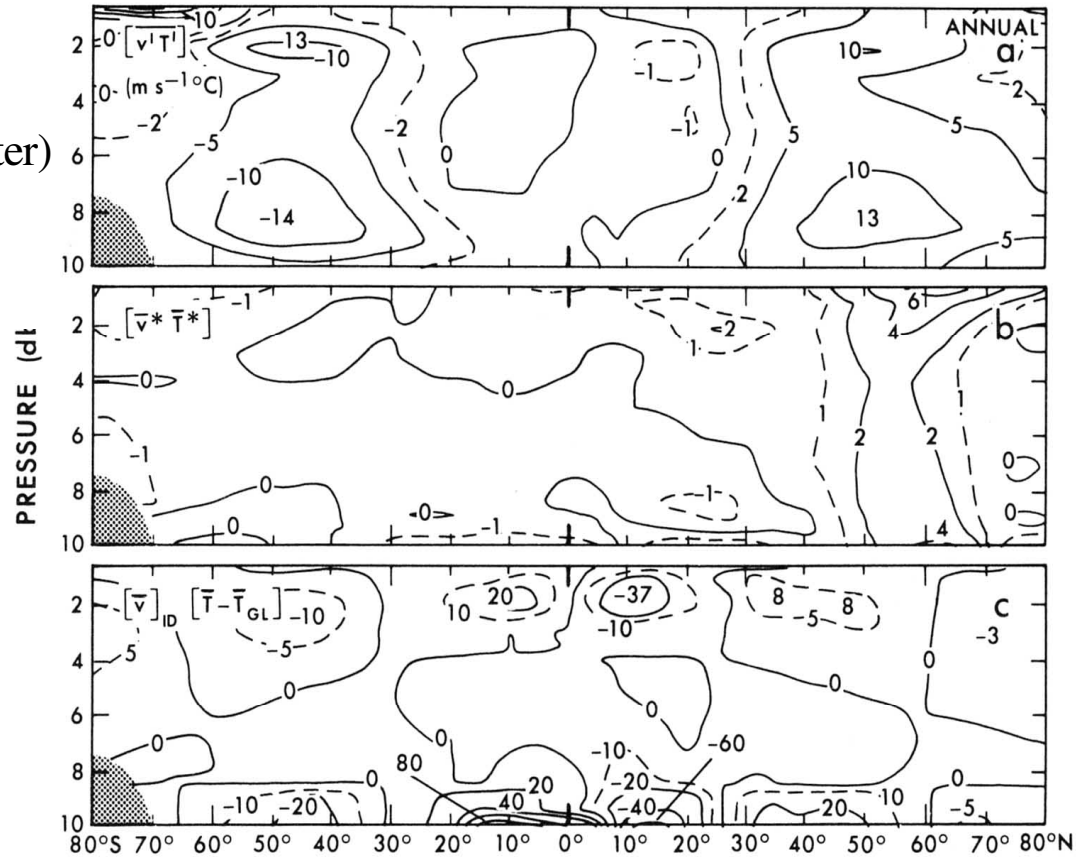


FIGURE 13.5. Zonal-mean cross sections of the northward transport of sensible heat by transient eddies (a), stationary eddies (b), and mean meridional circulations (c) in $^{\circ}\text{C m s}^{-1}$ (from Oort and Peixoto, 1983).

annual mean $\overline{u'v'}$:
 transient eddies dominate

[Oort & Peixoto]

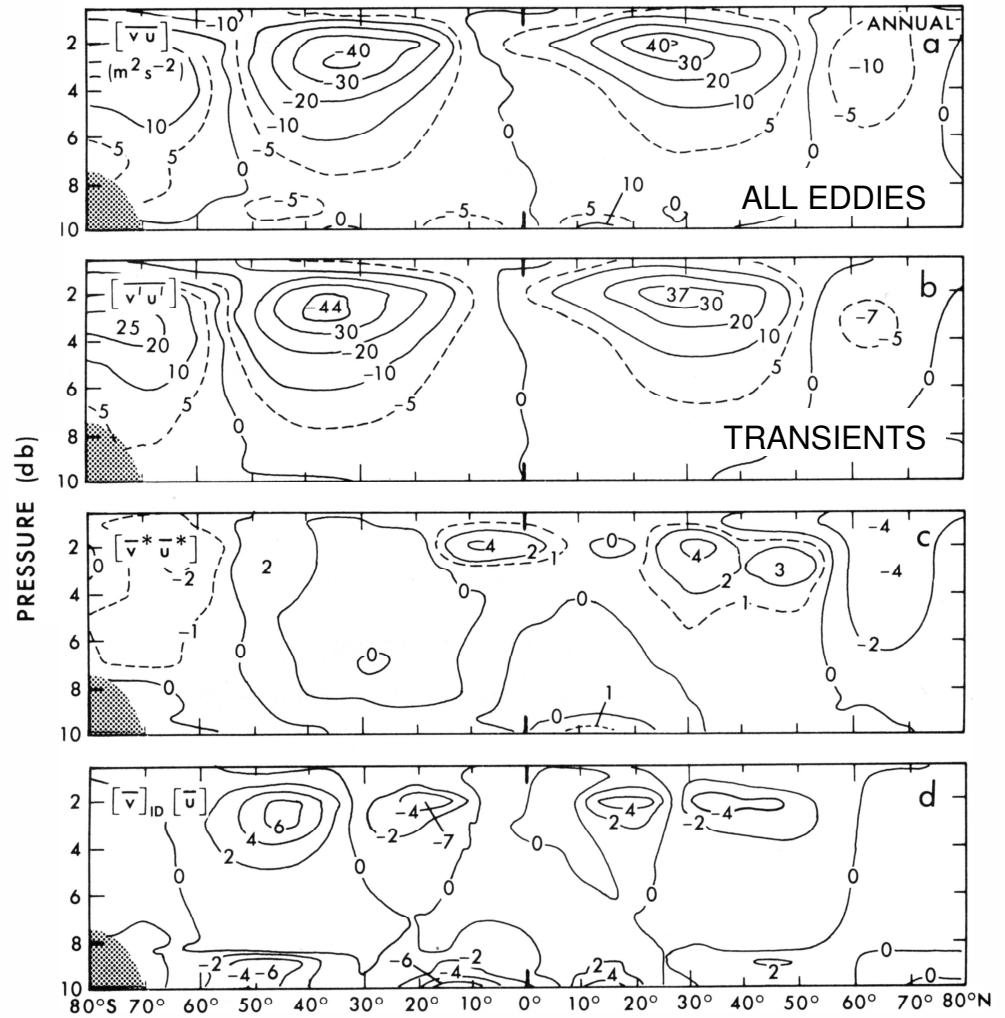
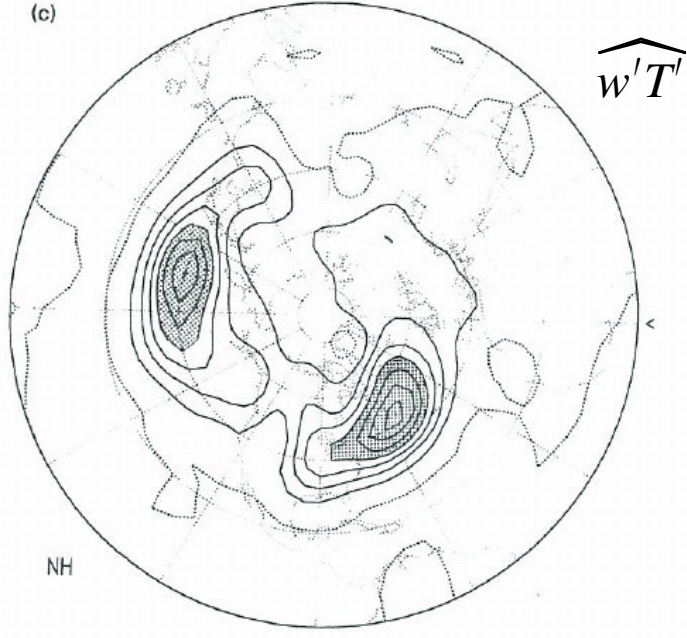
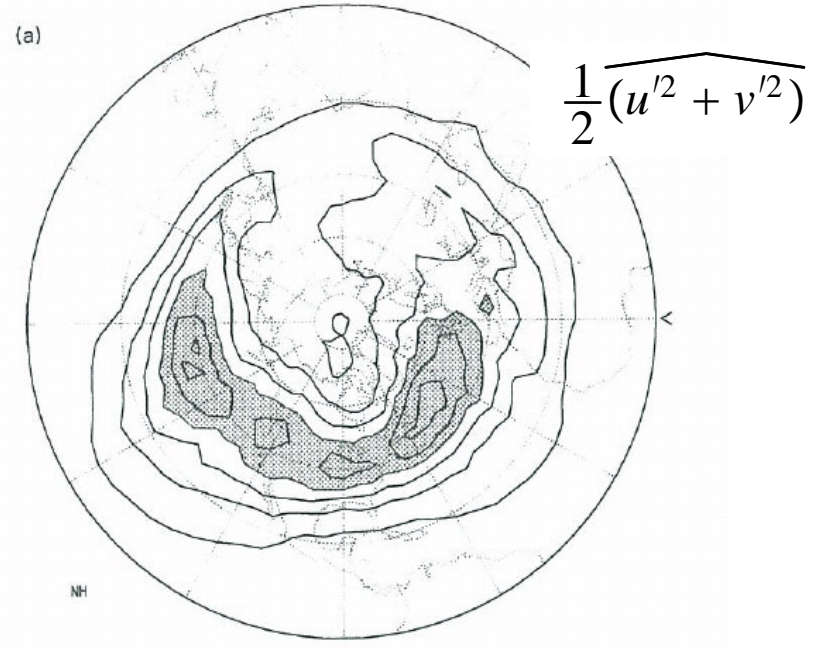
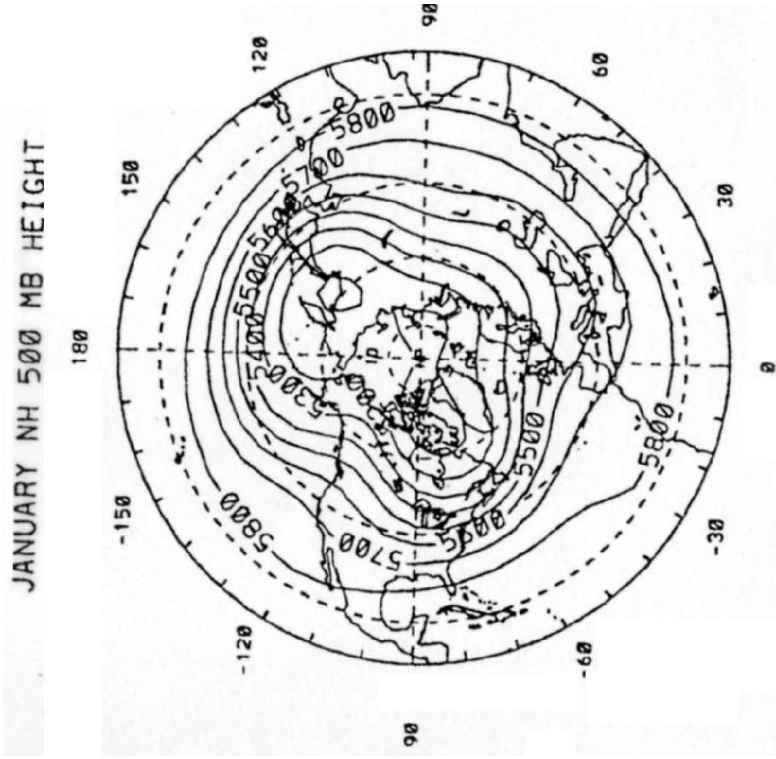
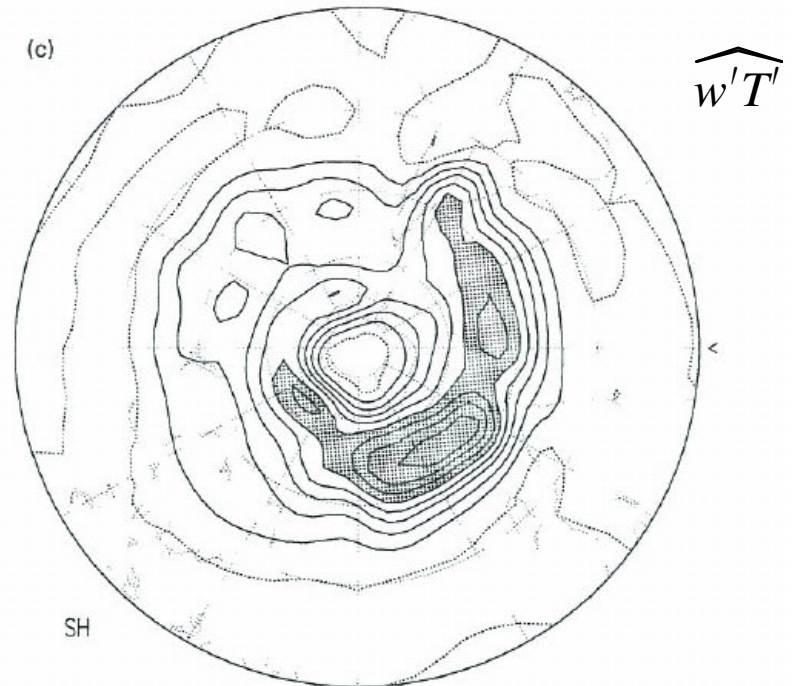
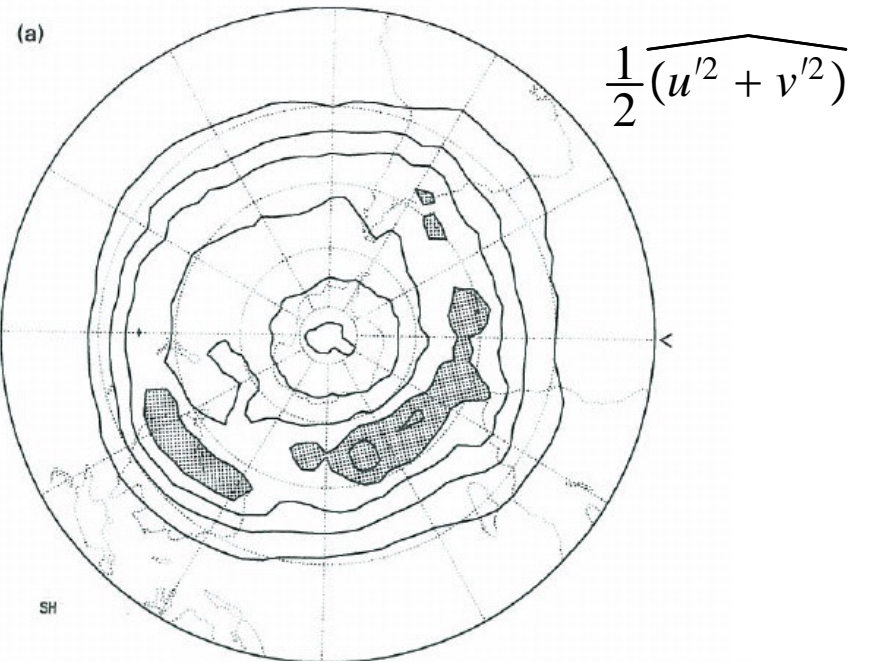


FIGURE 11.7. Zonal-mean cross sections of the northward flux of momentum by all motions (a), transient eddies (b), stationary eddies (c), and mean meridional circulations (d) in $\text{m}^2 \text{s}^{-2}$ for annual-mean conditions (from Oort and Peixoto, 1983).

Storm tracks – northern hemisphere

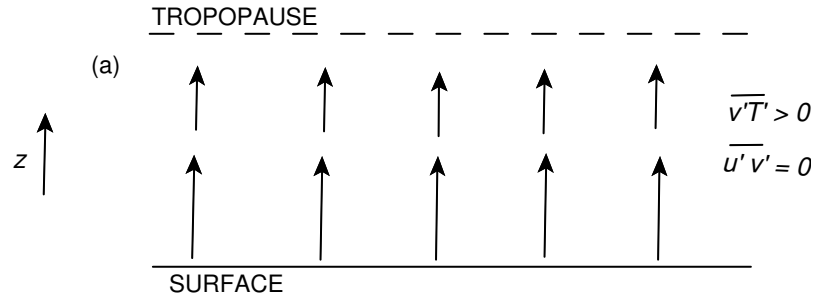


Storm tracks – southern hemisphere

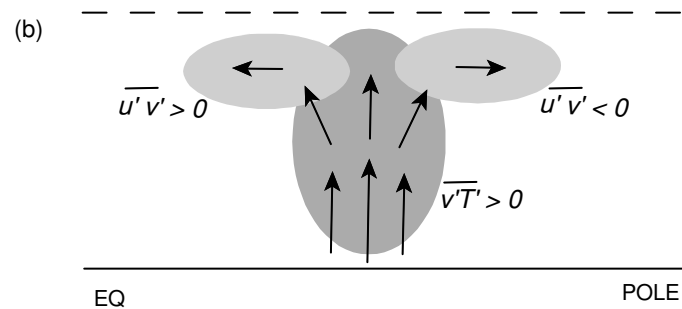


EP, heat and momentum fluxes
 (arrows show \mathbf{F})

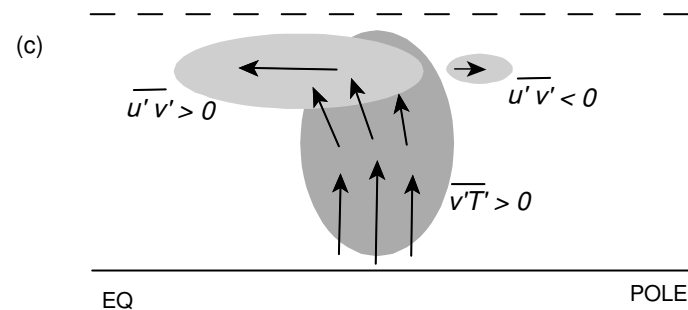
$$F^{(y)} = -\rho \overline{u'v'} ; \quad F^{(z)} = \rho f \frac{\overline{v'\theta'}}{\partial \bar{\theta} / \partial z}$$



homogeneous case $\overline{u'v'} = 0$



localized baroclinic zone on β -plane:
 wave activity spreads out symmetrically;
 $\overline{u'v'} \neq 0$



localized baroclinic zone on the sphere:
 wave activity spreads out asymmetrically;
 $\overline{u'v'}$ predominantly poleward

Maintenance of surface westerlies

column-integrated momentum budget:

$$-f\bar{v} = -\frac{\partial}{\partial y} \overline{u'v'} - \frac{1}{\rho} \frac{\partial \tau}{\partial z}$$

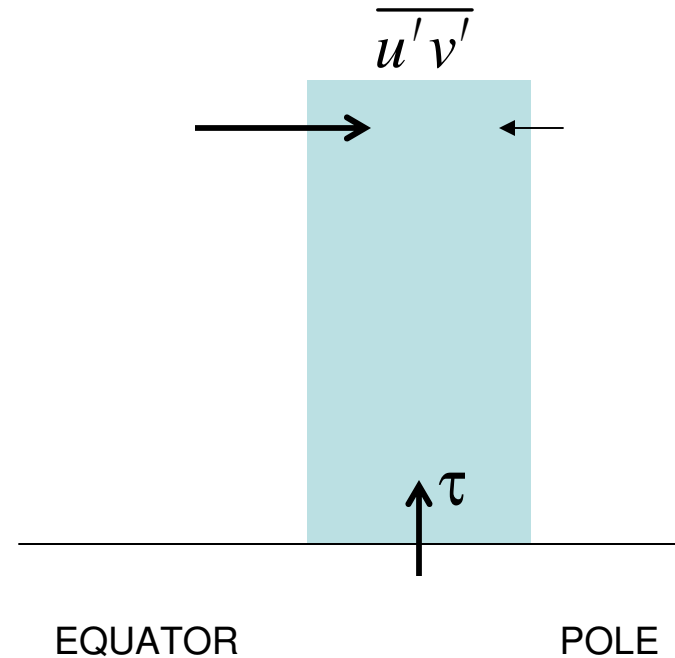
$$\rightarrow -f \int_0^{\infty} \rho \bar{v} dz = -\frac{\partial}{\partial y} \int_0^{\infty} \rho \overline{u'v'} dz + \tau_0$$

but $-f \int_0^{\infty} \rho \bar{v} dz = 0$

$$\rightarrow \tau_0 = \frac{\partial}{\partial y} \int_0^{\infty} \rho \overline{u'v'} dz$$

$$\tau_0 = -\frac{u_0}{\tau_{drag}}$$

$$\rightarrow \boxed{u_0 = -\tau_{drag} \frac{\partial}{\partial y} \int_0^{\infty} \rho \overline{u'v'} dz}$$



surface westerlies in middle latitudes (where momentum flux is convergent)

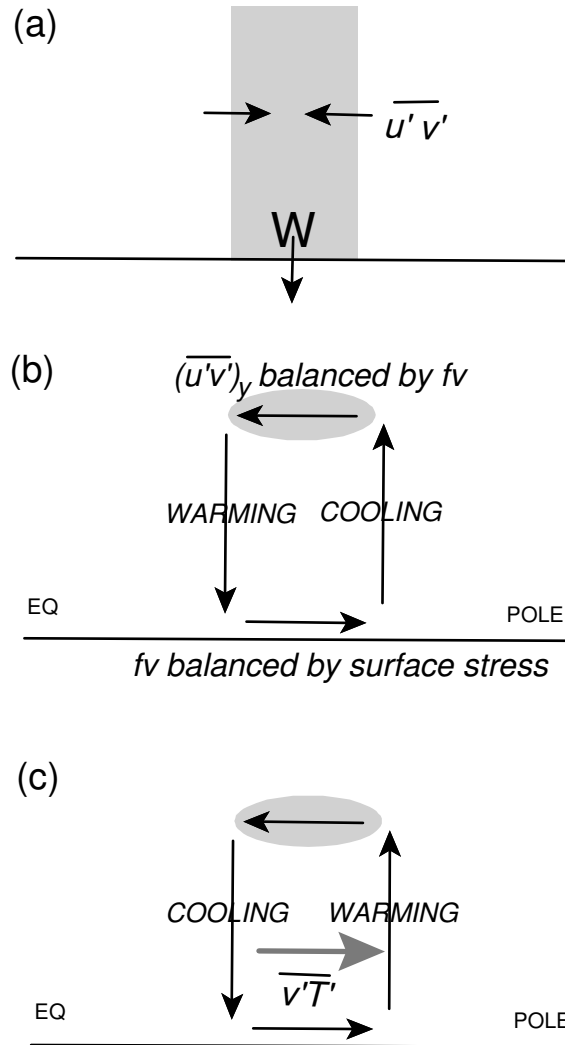
locally,

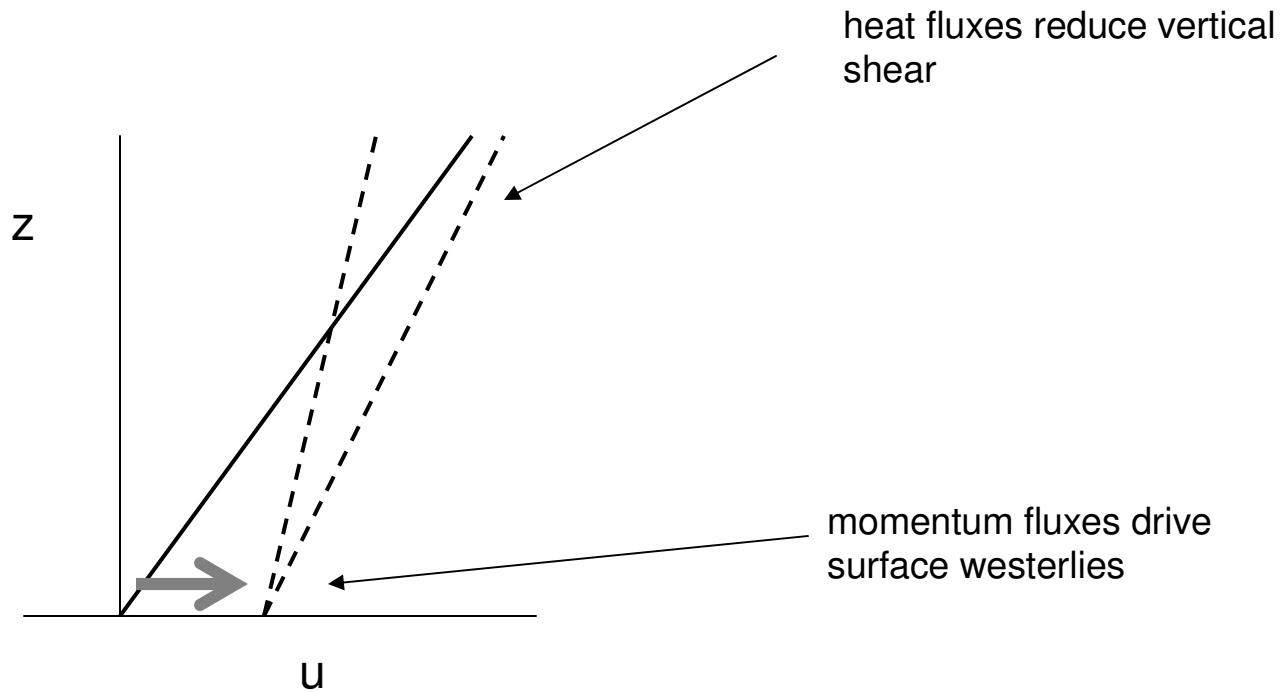
$$\bar{v} = \frac{1}{f} \frac{\partial}{\partial y} (\overline{u'v'})$$

→ Ferrel cell

heat transport by Ferrel cell opposes
(but does not overcome) effects of
eddy heat flux

→ net poleward heat transport





Whether eddies enhance or reduce upper tropospheric westerlies depends on external factors, such as ratio of thermal relaxation rate to surface drag coefficient [Robinson, *J Atmos Sci*, 1991]

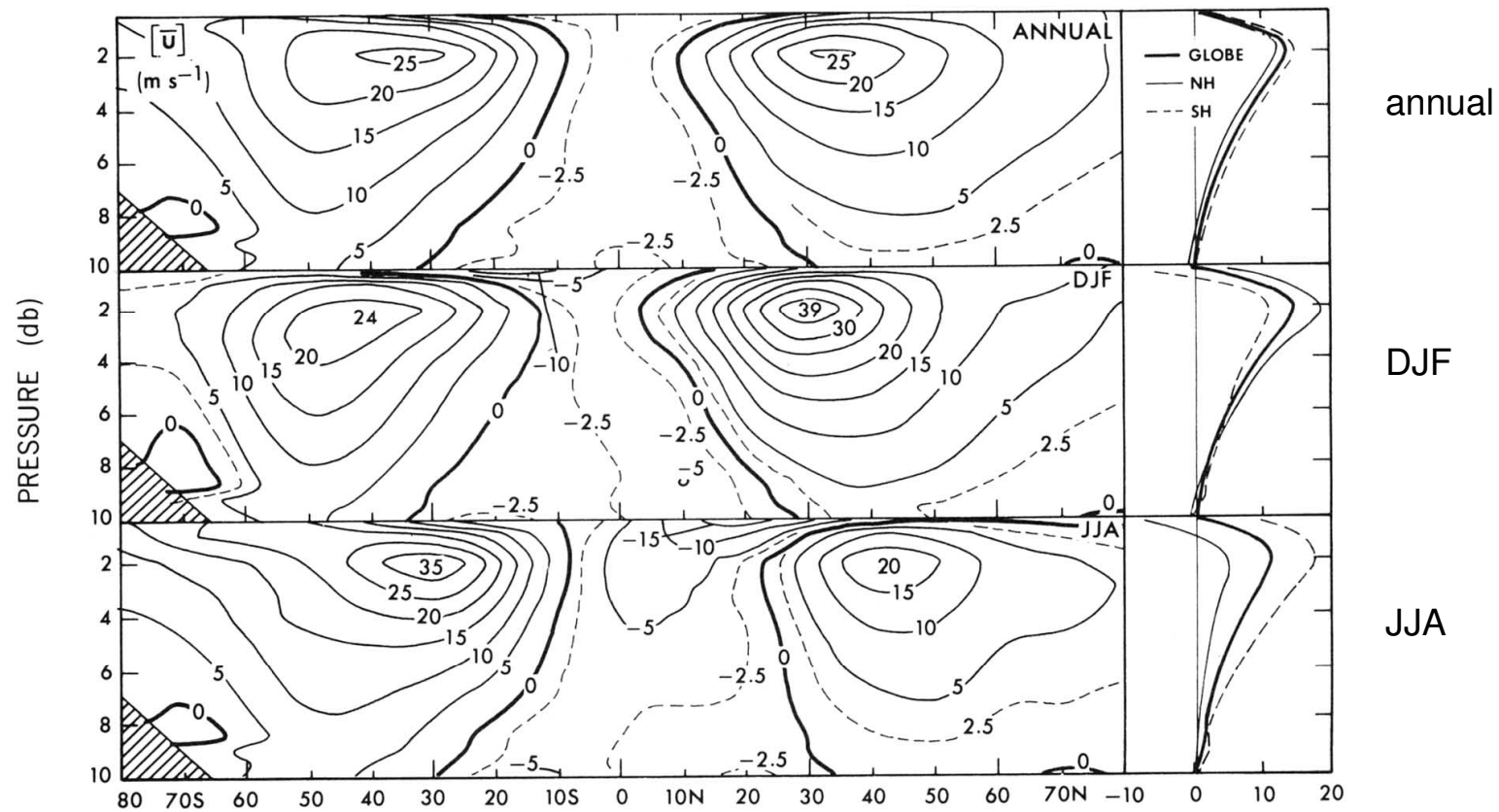
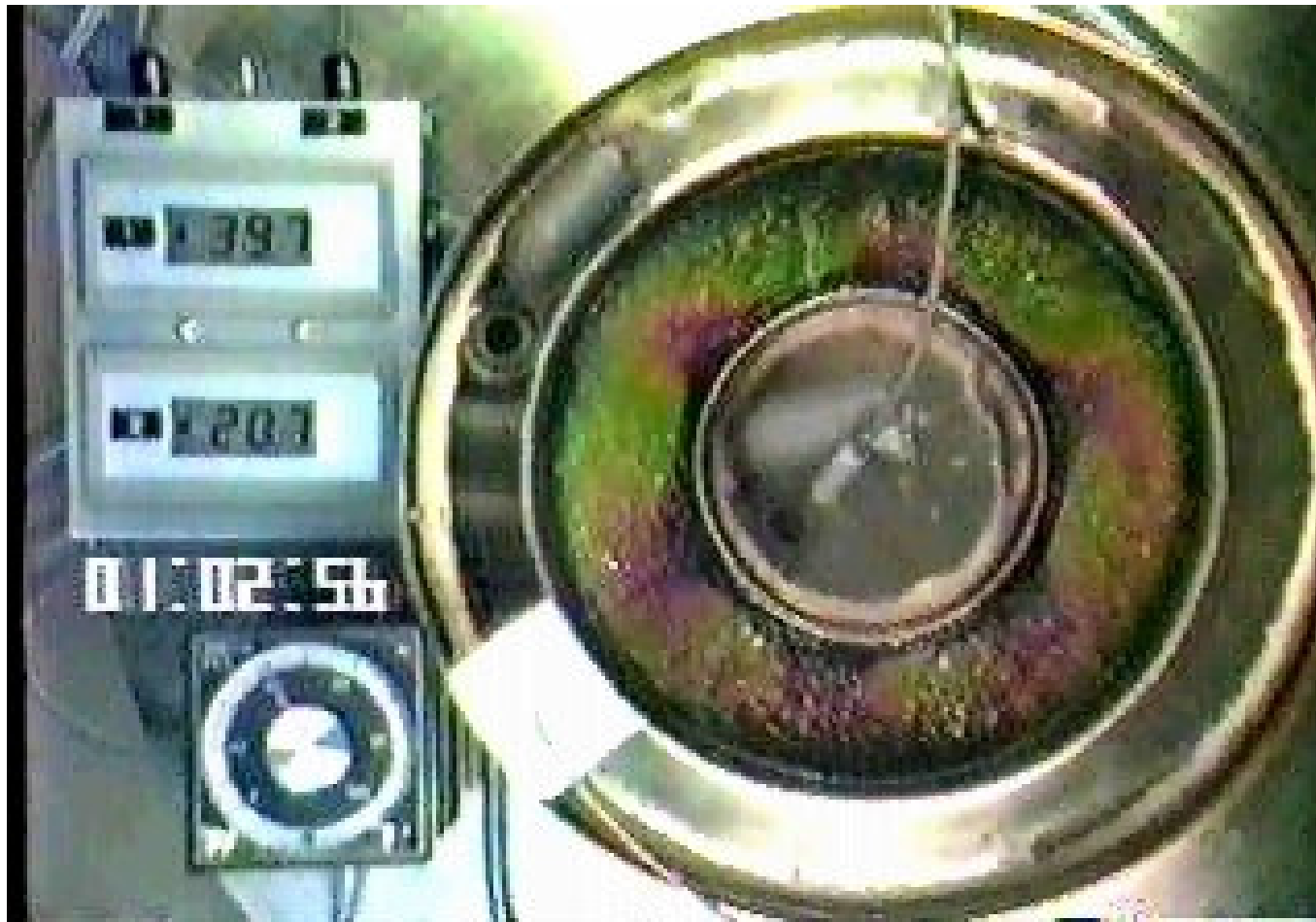


FIGURE 7.15. Zonal-mean cross sections of the zonal wind component in m s^{-1} for annual, DJF, and JJA mean conditions. Vertical profiles of the hemispheric and global mean values are shown on the right.

(vi) Variability: Annular modes

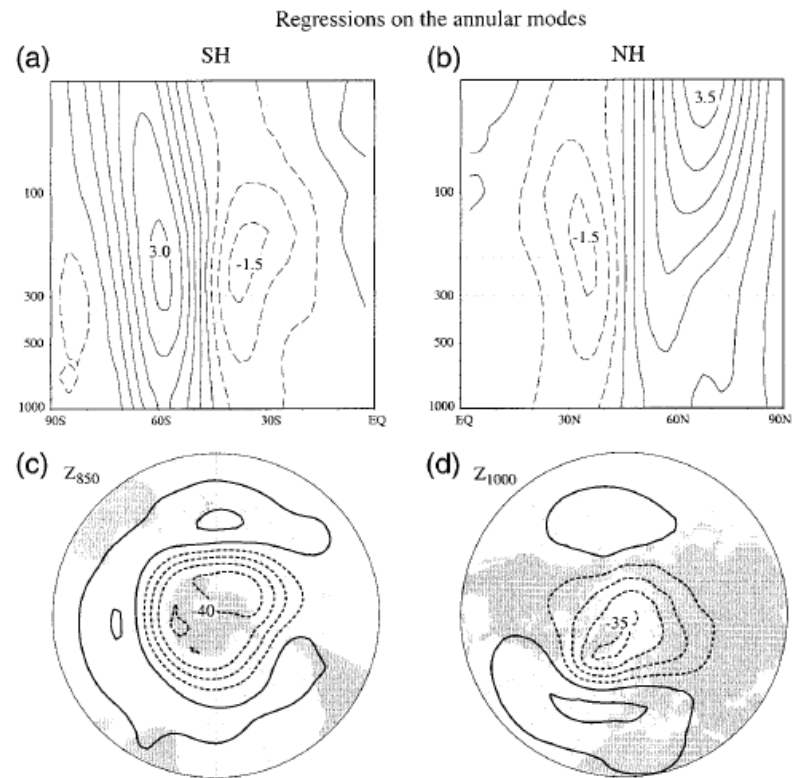
実験室の中の空と海

Atmosphere and Ocean
in a Laboratory



Annular Modes

- Leading patterns of variability in extratropics of each hemisphere
- Strongest in winter but visible year-round in troposphere; present in “active seasons” in stratosphere

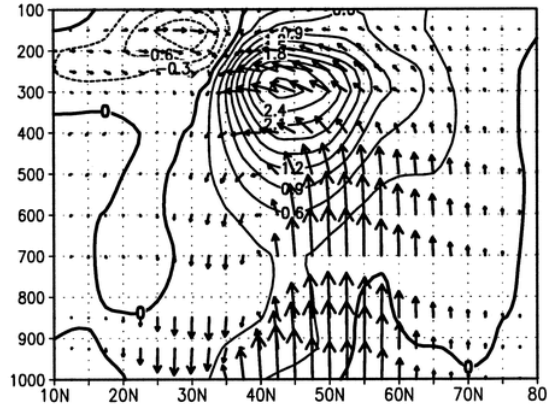


[Thompson and Wallace, 2000]

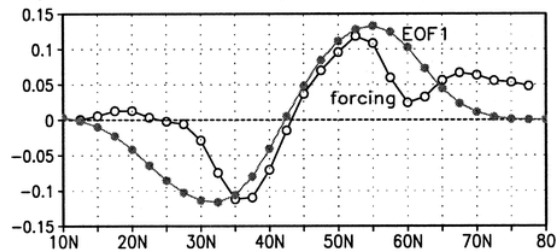
Lorenz & Hartmann

J. Atmos. Sci (2001); J. Clim (2003)

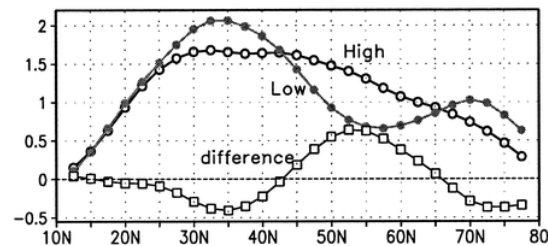
a) synoptic eddies ($u'v'$ & EP flux)



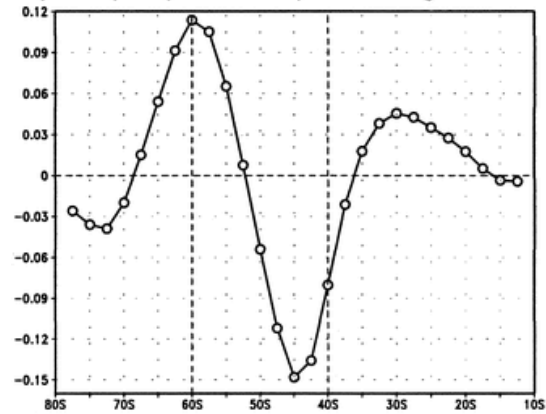
b) vert. ave. forcing & EOF1 pattern



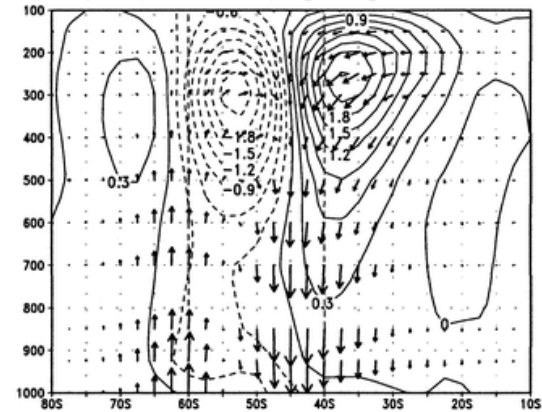
c) baroclinicity (700mb)



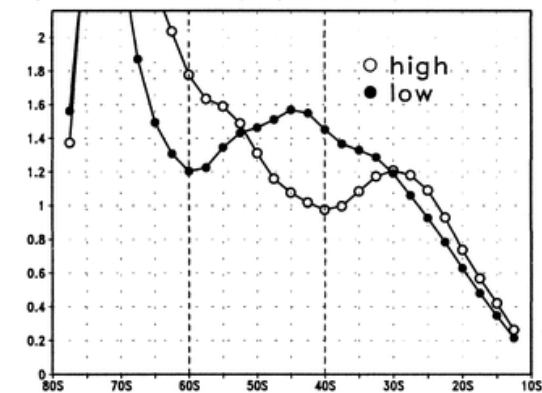
a) $\langle \text{synoptic eddy forcing} \rangle$



b) synoptic eddy [$u'v'$]



c) baroclinicity (850mb)



References

- Holton, J. R., 1992: An Introduction to Dynamic Meteorology Third Edition, Academic Press, 511pp.
- Lorenz, D.J. and Hartmann, D.L, 2001: Eddy--Zonal Flow Feedback in the Southern Hemisphere, J. Atmos. Sci., 58, 3312-3327
- James, I. N., 1995: Introduction to circulating atmospheres, Cambridge University Press, 448pp.
- Robinson, W. A., 1991: The dynamics of the zonal index in a simple model of the atmosphere, Tellus A, 43, 295-305
- Peixoto, J. P. and Oort, A. H., 1992: Physics of Climate. American Institute of Physics, 520pp.
- Held, I. M. and Hou, A. Y., 1980: Nonlinear Axially Symmetric Circulations in a Nearly Inviscid Atmosphere, J. Atmos. Sci., 37, 515-533
- Thompson, D. W. J. and Wallace, J. M. 2000: Annular modes in the extratropical circulation. Part I: Month-to-month variability, J. Climate, 13, 1000-1016
- NCEP,
<http://www.cpc.noaa.gov/>
- Atmosphere and Ocean in a Laboratory,
http://www.gfd-dennou.org/library/gfd_exp/index.htm